SOIL MECHANICS AND BITUMINOUS MATERIALS
RESEARCH LABORATORY

DESIGN CONSIDERATIONS FOR ASPHALT PAVEMENTS

by
C. L. MONISMITH
D. B. McLEAN
and
R. YÜCE

REPORT NO. TE 72-4

to
THE MATERIALS AND RESEARCH DEPARTMENT
DIVISION OF HIGHWAYS
STATE OF CALIFORNIA

PREPARED IN COOPERATION WITH
THE UNITED STATES DEPARTMENT OF TRANSPORTATION
FEDERAL HIGHWAY ADMINISTRATION

DEPARTMENT OF CIVIL ENGINEERING
INSTITUTE OF TRANSPORTATION AND TRAFFIC ENGINEERING

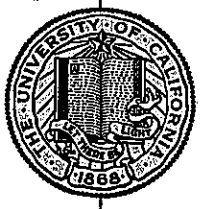

University of California · Berkeley

TECHNICAL REPORT STANDARD TITLE PAGE

1. REPORT NO.	2. GOVERNMENT ACCESSION NO.	3. RECIPIENT'S CATALOG NO.

4. TITLE AND SUBTITLE
Design Considerations for Asphalt Pavements

5. REPORT DATE
December 1972

6. PERFORMING ORGANIZATION CODE
19301-633153

7. AUTHOR(S)
Monismith, C. L., McLean, D.B., and Yüce, R.

8. PERFORMING ORGANIZATION REPORT NO.
TE 72-4

9. PERFORMING ORGANIZATION NAME AND ADDRESS
Office of Research Services
University of California
Berkeley, California 94804

10. WORK UNIT NO.

11. CONTRACT OR GRANT NO
D-6-1

12. SPONSORING AGENCY NAME AND ADDRESS
Department of Transportation
Division of Highways
Sacramento, California 95807

13. TYPE OF REPORT & PERIOD COVERED
Interim 10-1-71 to 12-31-72

14. SPONSORING AGENCY CODE
RTA 13945-191202 UCB

15. SUPPLEMENTARY NOTES
Conducted in cooperation with the U. S. Department of Transportation, Federal Highway Administration

16. ABSTRACT

A study to determine the applicability of using laboratory-determined fatigue response to predict the behavior of pavement slabs is presented.

Research in the permanent deformation area has been directed toward the development of equipment and procedures for testing specimens of asphalt concrete and soil in repeated loading to study their permanent deformation characteristics under representative environmental and loading conditions. Some preliminary results of tests on both types of materials are presented.

A preliminary framework for incorporating permanent deformation considerations into the pavement design process is also outlined.

17. KEY WORDS	18. DISTRIBUTION STATEMENT
Asphalt Pavements Fatigue Fatigue Tests Deformation permanent Resilient Modulus	Unlimited

19. SECURITY CLASSIF. (OF THIS REPORT)	20. SECURITY CLASSIF. (OF THIS PAGE)	21. NO. OF PAGES	22. PRICE
Unclassified	Unclassified	64	

HMRT - 1242 (ORIG. 9 72)

Soil Mechanics and Bituminous Materials

Research Laboratory

DESIGN CONSIDERATIONS FOR ASPHALT PAVEMENTS

A report on an investigation

by

C.L. Monismith

Professor of Civil Engineering and
Research Engineer

D.B. McLean
Research Assistant

and

R. Yüce
Research Assistant

to

The Materials and Research Department
Division of Highways
State of California

under
Research Technical Agreement 13945-191202 UCB
HPR-DR-1(9) D0601

Prepared in cooperation with
The United States Department of Transportation
Federal Highway Administration

Report No. TE 72-4, Office of Research Services
University of California, Berkeley, California
December 1972

INTRODUCTION

This report describes research completed during the 1971-72 period on the project concerned with design considerations for asphalt pavements. In addition a brief summary of current related research by other investigators is also included since it serves to complement research in this investigation and provides a basis for some of the effort undertaken in this research effort. Studies have continued in both the fatigue and permanent deformation areas.

In the fatigue area, a study to determine the applicability of using laboratory-determined fatigue response to predict the behavior of pavement slabs is presented.

Research in the permanent deformation area has been directed to the development of equipment and procedures for testing specimens of asphalt concrete and soil in repeated loading to study their permanent deformation characteristics under representative environmental and loading conditions. Some preliminary results of tests on both types of materials are presented.

A preliminary framework for incorporating permanent deformation considerations into the pavement design process (similar to that for fatigue) is also outlined.

SUMMARY OF RECENT RELATED STUDIES

During the past year the results of a number of studies have been presented which add useful information to the design process considered in this investigation and include efforts both in the areas of fatigue and permanent deformation.

Loading Times

A number of investigators have prepared guides to permit estimation of loading times for various materials comprising the pavement section (particularly important when assessing the stiffness of asphalt bound materials).

Analyses prepared by Barksdale (1) are shown in Figs. 1a and 1b. From these figures it can be seen that the time-of-loading is dependent not only on vehicle speed but also on the depth under consideration in the pavement section.

Brown (2) has used the work of Barksdale as well as other investigators to develop a procedure for defining an average stiffness for an asphalt bound layer considering the influence of layer thickness, vehicle speed, and temperature. An example of such a simplified representation for a dense graded mix with an 85-100 penetration asphalt cement is shown in Fig. 2. Similar relationships would necessarily have to be established for other types of mixes. Such an approach may be useful in the development of simplifications to design procedures of the type considered in this investigation.

Suggestions for loading times have also been made by a number of authors in their papers presented at the Third International Conference on the Structural Design of Asphalt Pavements and are summarized in Table 1. Interestingly, the times shown in the table are comparable to those developed by Barksdale (1) and Brown (2) and discussed above.

Fatigue

In report TE 70-5 some attempt was made to simplify the incorporation of fatigue in the pavement design process. Pell (8), Verstraeten (9), and Kirk (10) have suggested relationships wherein the effects of asphalt type and grade, amount of asphalt and void content of the mixture can be combined to define their relative effects on fatigue response without extensive testing.

Pell suggests that:

$$N(\text{at } \varepsilon = 10^{-4}) = P\left[\left(\frac{V_B}{V_B + V_v}\right)\left(T_{R\&B}\right)\right]^q \quad . \quad . \quad . \quad . \quad (1)$$

where

V_B = volume asphalt

V_v - volume of voids

$T_{R\&B}$ = Ring and Ball softening point temperature

P,q = coefficients

ε = tensile strain repeatedly applied

and that there exists a relationship between A and b of the fatigue equation

$$N_f = A\left(\frac{1}{\varepsilon}\right)^b \quad . \quad . \quad . \quad . \quad . \quad . \quad . \quad (2)$$

of the form:

$$b = f\ (\log A). \quad . \quad . \quad . \quad . \quad . \quad . \quad (3)$$

Data illustrating these relationships are shown in Figs. 3 and 4.

An analysis was made of previously reported fatigue data for California type mixes to determine the applicability of equation (3) for such mixtures. These results are shown in Fig. 5. Also included are values for the limiting curves of the generalized fatigue diagram from TE 70-5 (11) and shown here in Fig. 6, that is, for stiffnesses of 10^4 and 4×10^6 psi. Pell's relationship from Fig. 4 is shown for purposes of comparison. Such an approach may thus have merit.

The state of stress in a pavement resulting from traffic loading may be modified at times due to stresses resulting, for example, from temperature changes or shrinkage of the underlying layers. To interpret fatigue effects for such situations where alternating stresses are superimposed on continuously acting stresses, a more general form of the fatigue diagram, known as the Modified Goodman Diagram, can be used. Results of fatigue tests on one mix, (Containing Watsonville granite with a 1/2 in. maximum size and a medium grading) and plotted in this form are shown in Figs. 7 and 8 for tests at 10°F and 68°F.

To illustrate the use of such a diagram, a ratio representing the stress state is defined:

Stress State	R = min. stress/max. stress
Zero-to-maximum	0
Complete reversal	-1
Steady State	1
Tension-tension or compression-compression	0<R<1

The abscissa on the diagram represents the minimum stress and the ordinate the maximum stress. Thus the equations R = ±1 are represented by straight

lines inclined at 45° to the maximum and minimum stress coordinates. The equation of R = 0 is represented simply by the ordinate while the static strength is represented as a point on the line R = 1. Zero-to-maximum stress associated with a given fatigue life falls on the R = 0 line whereas complete reversal is represented by the line R = -1.

It is also possible to superimpose on the lines R = 1 and R = -1, scales representing the mean stress and the alternating stress. When the mean stress is zero, complete reversal occurs (R = -1); when the mean and alternating stresses are equal, the zero-to-tension condition results (R = 0); and when the alternating stress is zero, the static strength is obtained (R = 1).

Accordingly, this type of diagram appears to be a very general and useful form that can be used for representing a wide spectrum of stress combinations which may occur in pavements.

An additional advantage is that fatigue lines plot practically as straight lines for many materials; thus an entire relationship could be obtained from knowledge of the static strength and fatigue data obtained for the condition R = 0 (i.e., the conditions for which all the data presented in preceding paragraphs were obtained).

Permanent Deformation (Distortion)

Barksdale (12) has examined the accumulation of permanent deformation in unbound granular materials subjected to repeated loading triaxial compression tests and has suggested a procedure whereby the results of such tests can be used to estimate rutting in pavement sections containing these materials. Romain (13) has also described a process to estimate permanent deformations in layered elastic systems which is similar to that suggested by Barksdale.

The results of Barksdale's laboratory repeated load tests follow a hyperbolic stress-strain law of the form:

$$\epsilon^p = \frac{(\sigma_1 - \sigma_3)/K\,\sigma_3^n}{1 - \left\{\frac{(\sigma_1 - \sigma_3)R_f(1 - \sin\phi)}{2(c\cos\phi + \sigma_3 \sin\phi)}\right\}} \quad . \quad . \quad . \quad . \quad . \quad . \quad (4)$$

where:

$K\,\sigma_3^n$ = relationship defining the initial tangent modulus as a function of confining pressure

c = cohesion

ϕ = angle of internal friction

R_f = constant relating compressive strength to an asymptotic stress difference; $0.75 \leq R_f \leq 1$

Alternatively, letting $\bar{\sigma} = (\sigma_1 - \sigma_3)$ - the effective stress difference in triaxial compression and $\bar{\epsilon}^p = \epsilon_1$ (for the condition with $\epsilon_1 + \epsilon_2 + \epsilon_3 = 0$),

$$\frac{\bar{\epsilon}_p^p}{\bar{\sigma}} = \frac{1/K\,\sigma_3^n}{\left\{1 - \frac{\bar{\sigma}R_f\,(1 - \sin\phi)}{2(c\cos\phi + \sigma_3 \sin\phi)}\right\}} \quad . \quad . \quad . \quad . \quad . \quad . \quad . \quad (5)$$

Fig. 9 illustrates a comparison of actual test results with those estimated using a hyperbolic relationship.

From an examination of Barksdale's data, Freeme (14) has suggested that:

$$\frac{\bar{\varepsilon}^p}{\bar{\sigma}} = \left[\frac{1/K\sigma_3^n}{1 - \frac{\bar{\sigma}R_f\ (1 - \sin\phi)}{2(c\cos\phi + \sigma_3 \sin\phi)}} \right] \left(\frac{N}{N_o}\right)^A \quad . \quad . \quad . \quad (6)$$

where the parameters in equation (6) are determined at N_o repetitions of load. This is also illustrated in Fig. 9.

To predict the amount of rutting, each layer of the pavement structure is subdivided into several sublayers. The major principal stress and average confining pressure are calculated at the center of each layer beneath a wheel as shown in Fig. 10. Barksdale recommends that the stresses be estimated using a non-linear theory to recognize the non-linear anisotropic behavior of untreated base materials. For a specific number of load repetitions, the plastic strain can then be readily ascertained from equation (6) (or directly from the laboratory curve). The total rut depth may be determined by summing the products of the average plastic strains occurring at the center of each layer and the corresponding layer thickness (Fig. 10), i.e.,

$$\delta^p = \sum_{i=1}^{n} (\bar{\varepsilon}_i^p \cdot h_i) \quad . \quad . \quad . \quad . \quad . \quad (7)$$

where:

δ^p = rut depth

$\bar{\varepsilon}_i^p$ = average plastic strain

h_i = layer thickness

As will be seen subsequently this type of an approach is recommended as a part of the subsystem used to estimate distortion due to repetitive loading (Fig. 27).

Romain has suggested a similar approach and has recommended that the stresses be computed using multilayer elastic theory*. In Romain's approach consideration is given to loads applied to dual as well as single tires and to the lateral distribution of traffic across the pavement section. In addition the contribution of the subgrade to rutting is limited to a depth of 3 meters below the subgrade surface.

Both of these studies thus lend support to the procedure to be described subsequently.

---

*Romain has noted (13): "....an earlier investigation of the author's (Romain's) has shown that the stress distribution in a viscoelastic layered system under brief enough solicitations (such as those induced by a moving vehicle) is quite acceptably approximated, for engineering purposes, by that in an elastic layered system with time dependent moduli....."

SLAB TEST STUDY

While previous studies have made use of laboratory determined fatigue data to estimate field performance (11), some concern exists as to the appropriateness of such methodology since the state of stress which is developed in the conventional laboratory test is generally uniaxial (15), while that which exists in the field is multiaxial. Moreover, the influence of crack propagation times on fatigue lives in laboratory tests may be different than that for mixes in in-service pavements. For these reasons the study described in this section was conducted, the major objective being to ascertain whether or not laboratory determined fatigue data could be used to predict the cracking which might be developed in slab specimens subjected to repetitive loading under controlled environmental and loading conditions.

The procedure followed in this study is, admittedly, a very direct procedure and is only one of a number of alternatives which are available. One falling into the latter category is that which is being developed by Majidzadeh (16) using principles of fracture mechanics. Presumably such methodology holds promise to be incorporated into fatigue design to predict the areal extent of cracking. Before this can be accomplished, however, considerable research appears necessary (17).

Materials

An 85-100 penetration asphalt cement supplied by the Chevron Research Company and Watsonville granite were used to prepare the slab test specimens. For the 3/8 in. maximum size aggregate grading used (fine grading), Fig. 11, an asphalt content of 5.8 percent* (by weight of aggregate) was estimated by the State of California procedure (18) which was increased (for convenience) to 6.0 percent for the test specimens.

Properties of the recovered asphalt contained in the slabs at the time of test were:

penetration at 25°C	31 dmm
ring and ball softening pt	143.5°F

Slab Test Specimen Preparation

The mix for the slab test specimens was mixed in a Barber Greene "Mixall"** (300 lb batch) for about 3 minutes at a temperature of 300+°F.

Specimens were compacted in the forms shown schematically in Fig. 12 using a vibratory compactor. Fig. 13 illustrates this process as well as the technique used to determine the thickness of the compacted slab.

---

* Surface area of aggregate = 49.4 sq ft per lb, k_m = 1.15.

** The mixer was loaned to the University by the Chevron Research Company.

Following compaction the specimens were sawed into specimens 39 in. by 39 in. plan. The 21 in. sections remaining at one end of each of the slabs were used to obtain specimens for fatigue testing.

A total of 12 slabs were prepared in this manner. Table 2 contains a summary of the height, unit weight, and void content for each of the slabs.

Slab Testing

Equipment Each of the slabs was tested on a spring base simulating an elastic foundation (approximately 1600 springs) developed by Secor (19) which could be placed in a controlled temperature environment (40°F - 140°F range). Repeated loads were applied to a 2 in. circular area at the center of the slabs by means of pneumatic loading unit at a frequency of 100 repetitions per minute and for a duration of 0.1 sec. Fig. 14 shows a view of the base plus one of the loading units.

Tests were conducted using two different moduli of subgrade reactions, 200 psi and 57 psi respectively (achieved by using springs with different constants).*

Instrumentation. To measure strains and the onset of cracking in the slabs under repetitive loading SR-4 type strain gages, aluminum foil tape and silver conducting paint were bonded to the slabs in patterns similar to that illustrated in Fig. 15.

Gages were first bonded to the bottom of the slab (Fig. 17); the slab was then placed on the spring base using a vacuum technique as shown in Fig. 16a and 16b. Additional strain gages were bonded to the top of the slab after it was in place on the spring base.

Deflections were measured using linear variable differential transformers.

---

*These spring constants cover a range in subgrade stiffnesses from what would be considered high to low.

Test Procedure Prior to testing, each slab was allowed to remain at the temperature of test (achieved by an insulated cover surrounding the spring base) for 24 hours.

Load was applied pneumatically for a period of 0.1 sec and at a frequency of 100 repetitions per minute. Strains and deflections were recorded periodically on a Sanborn strip-chart recorder.

By observing the recorder records, crack initiation and propagation could be ascertained. Generally each test was continued until a substantial increase in the deflection under the load was observed.

Of the twelve slabs tested in the investigation, 10 were tested with the instrumentation shown in Figs. 17 and 18 while two were tested without instrumentation to investigate the influence of the size of the loaded area and the adhesive on the final crack pattern.

Test Results. A summary of the test conditions for the twelve slab tests are presented in Table 3.

Stiffness measurements on beam specimens from slab specimens obtained near the loaded area were performed following the repetitive loading slab tests. These results are shown in Table 4 and are based on deflections obtained after 200 stress applications applied at a frequency of 100 per minute and for a duration of 0.1 sec.

As noted earlier, deflections and strains were recorded during the course of each test. Fig. 19 illustrates the change in deflection with number of stress applications for slabs 3 through 10. It will be noted that the deflection for a particular slab remains relatively constant for a number of repetitions then increases relatively quickly as the slab cracks. This change in deflection for each slab will be related to the number of applications to failure subsequently.

Slab stiffnesses were also estimated from the equation:

$$S(t,T) = \frac{3P^2 (1 - \nu^2)}{16\ h^3 .\ k\ .\ z^2} \quad . \quad . \quad . \quad . \quad . \quad . \quad . \quad (8)$$

where:

$S(t, T)$ = slab stiffness* at specific time of loading and temperature

P = applied load (peak value)

ν = Poisson's ratio**

h - slab thickness

k = modulus of subgrade reaction

z = center deflection

Computed changes in this stiffness with number of load applications are shown in Fig. 20 for Slabs 4, 5, and 6, and in Fig. 21 for slabs 7 - 10.

The plots were used to provide estimates of the number of load applications to failure, defined as the number of repetitions in the vicinity of the change in slope of the deflection or stiffness vs. repetitions relationships.

---

* This stiffness corresponds to the elastic modulus for the elastic solution.

** Values for Poisson's ratio were determined from direct tension tests.

Estimates of cracking were also provided by the sensors attached to the bottom of each slab. The silver conducting paint appeared to provide some measure of "hair-line" cracking on the bottom of the slabs because of its brittle nature which may or may not be related to crack initiation of major fatigue cracks. The aluminum foil tape on the other hand appears to reflect relatively large failure cracks (1-2 mm in size).

Numbers of repetitions to failure (or first cracking) as estimated by the procedures described above are summarized in Table 5. Because the change in shape of the deflection and stiffness vs stress application relationships is not so well defined at the lower applied stress levels, ranges in stress application rather than single values are shown in the table.

Formation of each pattern in each of the stresses was determined by the use of a Sanborn event recorder. Prior to load application each crack sensor element was represented by a separate continuous straight line on the recording chart of the event recorder. A failure in one of the crack sensors resulted in a broken line on the strip chart. Initial cracking and the subsequent spread of cracking could be followed with this equipment. The final crack pattern observed in all instrumented slabs is illustrated in Fig. 22; Fig. 23 illustrates cracking through the silver conducting paint.

Because the size of the circular crack was about the same size as the 2.0 in diameter loading foot a slab was tested with a 5.0 in. diameter loading foot at the same stress level. In this instance the crack pattern was slightly larger in diameter, approximately 2.5 in. vs 2.0 in. in the previous tests. Fig. 24 illustrates the crack pattern for this test.

Another slab was tested without instrumentation to ascertain the influence of the epoxy adhesive used to bond the gages to the slab on final crack pattern. At the conclusion of this test, inspection of the crack pattern indicated that the radial cracks extended to the center of the loading foot rather than stopping at the circumferential crack as in the previous slab tests indicating that the epoxy adhesive used to bond the rosette gages directly under the loading foot had provided some stiffening effect by not allowing the radial cracks to form under the loading foot.

Analyses

While the primary purpose of this study was to determine the applicability of the use of laboratory determined fatigue data to predict the number of repetitions associated with cracking in the slabs, the data also provided an evaluation of the ability of theory to predict deflections. Both aspects will be discussed in this section.

Table 5 contains, in addition to the number of load applications associated with cracking from the slab measurements, an estimate of the number of applications to failure determined from fatigue tests

on the beam specimens. As will be seen in the table, the laboratory fatigue test results appear suitable to predict the slab response. This point is more clearly demonstrated in Fig. 25 where the mean fatigue curve plus the scatter band for the laboratory tests are shown, with the data from Table 5 superimposed.

Deflections, for comparison with measured values, were estimated from solutions for a uniform circular load applied to the surface of a plate on a dense liquid subgrade (20) (Fig. 26) namely:

$$z = \frac{p_o}{k} \left\{ 1 + \frac{\pi}{2} I_m \left[\mu H_1^* (\mu) \; J_o (\lambda r) \right] \right\} \quad \text{for } r \leq a \quad . \quad . \qquad (9)$$

and

$$z = \frac{p_o}{k} \left\{ \frac{\pi}{2} I_m \left[\mu J_1 (\mu) \; H_o^* (\lambda r) \right] \right\} \quad \text{for } r > a \quad . \quad . \quad . \qquad (10)$$

where:

J_o, J_1, H_o and H_1 are Bessel and Hankel functions

$$\lambda = e^{i \frac{\pi}{4}} \sqrt[4]{\frac{k}{D}}$$

$$\mu = \lambda a$$

In the deflection computations, the stiffness values of the beam specimens sawed from the slabs (0.1 sec loading time, 68°F) and presented in Table 4 were used. Poisson's ratio was assumed to be 0.5 based on a series of tests conducted in direct tension.

The results presented in Table 6 lend further support to the use of elastic theory to predict response of asphalt materials in repetitive loading provided the appropriate stiffnesses of the asphalt bound materials (as a function of temperature and time of loading) are used.

DISTORTION SUBSYSTEM

Some progress has been made in developing elements of the distortion subsystem shown in Fig. 27. Primary effort has been directed to development of test procedures to determine the distortion characteristics (Block No. 10) of both fine-grained subgrade soils and asphalt concrete mixtures. Some consideration has also been given to the structural analysis phase (Block No. 9).

Structural Analysis and Distortion Prediction (Block No. 9 and 11)

At this time, and essentially as suggested by Barksdale and Romain, it is recommended that stresses be ascertained using an elastic analysis. Available programs include: solutions for a multilayer elastic system CHEV 5L (21), CHEV 5L W/ITERATION (11), BISTRO (22), and ELSYM 5 (23); or a finite element solution such as FEPAVE 2 (11). Thus far the effort has been limited to use of solutions for a multilayer elastic system. This procedure also requires that some relationship between plastic strain and the applied stress state be available, i.e.,

$$\varepsilon^p = f(\sigma_{ij}) \quad . \quad . \quad . \quad . \quad . \quad . \quad . \quad . \quad (11)$$

With such a relationship it is then possible to estimate the permanent deformation which occurs in a particular pavement layer. This is done by computing the permanent strain at a number of points within the layer, the number being sufficient to reasonably define the strain variation with depth. The permanent deformation is then determined by summing the products of the average

permanent strains and the corresponding difference in depths between the locations at which the strains were determined (Fig. 28) i.e.:

$$\delta_i^p (x,y) = \sum_{i=1}^{n} (\varepsilon_i^p \Delta z_i) \quad . \quad . \quad . \quad . \quad . \quad . \quad . \quad (12)$$

where:

$\delta_i^p (x,y)$ = rut depth in the ith position at point (x,y) in the horizontal plane

ε_i^p = average permanent strain at depth $(z_i + \frac{\Delta z_i}{2})$

Δz_i = difference in depth

Total rut depth may be estimated by summing the contributions from each layer.

This analysis follows the same format as that for the fatigue subsystem described in earlier reports.

Material Characterization (Block No. 10)

To measure the permanent deformation characteristics of the various materials comprising the structural pavement section requires that the materials be tested under representative service conditions. For asphalt concrete specimens this requires at least that realistic states of stress, times of loading and temperatures be utilized. For untreated subgrade soils (at specific dry densities and water contents), stress state and time of loading would appear to be of primary concern. In this investigation procedures to study both types of materials have been developed and will briefly be described in this report.

Subgrade Soil. From a series of analyses (e.g., 12, 24) it would appear reasonable to use a square wave pulse of the type used previously to measure resilient moduli (25). In addition, from an examination of Barksdale's data (Fig. 1) the 0.1 sec loading time utilized in moduli determinations would appear quite reasonable to represent the average of a range in vehicle speeds at reasonable depths for subgrades. On this basis, therefore, a program has been initiated to measure the permanent deformation characteristics of subgrade soils. Appendix A contains a description of the laboratory procedure which has been developed.

Some tests have been performed on laboratory compacted specimens of the subgrade soil from Ygnacio Valley Road (11) in Contra Costa County. Water contents and dry densities of test specimens prepared by static compaction (10) are shown in Fig. 29.

Results illustrating the accumulation of permanent axial strain are shown in Fig. 30. It would appear that an equation of the form:

$$\varepsilon_i^p = AN^b \quad . \quad . \quad . \quad . \quad . \quad . \quad . \quad (13)$$

where a, b = experimentally determined coefficients

can be used to estimate the accumulation of permanent strain with number of stress applications. Preliminary data indicate that the coefficient A is dependent on at least the water content of the specimen as well as the repeatedly applied axial stress.

These same preliminary studies indicate that a hyperbolic relationship as suggested by Barksdale for granular materials may also represent the influence of axial stress level on the amount of permanent strain at a particular number of stress applications, i.e.,

$$\Delta\sigma_1 = \frac{\varepsilon_1^p}{\ell + m\,\varepsilon_1^p} \qquad (14)$$

where:

$\Delta\sigma_1$ = repeatedly applied axial stress

ℓ,m = experimentally determined coefficients

Data analyzed in this manner are shown in Fig. 31 for the relationship between deviator stress and axial permanent strain corresponding to 10,000 stress applications.

This type of data should be useful in the estimation of permanent deformation (Block 11, Fig. 27) when the state of stress has been ascertained.

Asphalt Concrete. To examine the accumulation of permanent deformation in thick layers of asphalt concrete subjected to repetitive loading requires more extensive characterization procedures than for subgrade soils to represent the multiplicity of loading and temperature conditions which will be obtained in-situ.

McLean (24) has prepared an analysis* of the loading and temperature conditions which might be utilized to examine such response. The factors which he examined include:

1. range of boundary stresses
2. distribution of stresses within the layer
3. stress-time relationships

---

* The analysis was conducted on a multilayer elastic system in which the properties of the materials were varied to reflect their non-linear response characteristics.

The magnitude of applied stresses resulting from loads applied by dual tires generally lies within the shaded areas shown in Figs. 32a and 32b.*

Examination of the variation of stress at a point due to placement of the load at varying distances from the point provides an indication of the shape of stress-time relationship to be used. Based on McLean's analysis, recommended shapes are shown in Table 7. Also included in this table are suggestions for the stress conditions to be utilized.

Time of loading data, Fig. 33 and referenced in Table 7, indicate that the horizontal stress is, in many cases, of longer duration than the vertical. This factor may exert a substantial influence on the deformation characteristics of asphalt concrete.

To recognize the different loading conditions which might occur, it was decided to use the repeated load triaxial compression equipment developed by Dehlen (26). This equipment permits independent application of axial and radial stresses in repeated loading. Some modification of the loading system was required to permit different shapes for the load pulses and differences in loading times. Appendix B contains a brief description of the equipment and the procedures used to test asphalt concrete specimens in repeated loading.

As in the earlier investigations, simplification of test procedures is most desirable, particularly if a subsystem of the type shown in Fig. 27 is to be implemented. Accordingly, consideration has been given to creep testing as well as repeated load testing of asphalt concrete. At present the results of creep tests can be used in a solution of a lyered viscoelastic solid proposed by the Federal Highway Administration (FHWA) to estimate

---

* The modular ratio used in this figure, G_1/G_2, is the ratio $\frac{E_1(1+\nu_2)}{E_2(1+\nu_1)}$.

rutting (BESYS II (27)); and it is possible that such tests may eventually be used in other analysis procedures for the same purpose.

At the time of this report only preliminary repeated load testing has been completed. Results of tests over a range in temperatures are shown in Figs. 35 through 37. It will be noted that the shapes of the strain vs. number of stress application curves are essentially the same regardless of the type of test used to induce the permanent deformation.

A number of analyses are available to permit development of relationships from the data which can be used for estimation of rutting in pavement structures.

One procedure consists of fitting a third order polynomial of the form:

$$\log \varepsilon^p = C_0 + C_1 \log N + C_2 (\log N)^2 + C_3 (\log N)^3 \quad . \quad . \quad (15)$$

to data of the type shown in Figs. 35 through 37. The influences of stress state, time of loading, and temperature are reflected in the coefficients C_0, C_1, C_2, and C_3.

Another procedure which has potential would utilize the theory of rate dependent plasticity (28). This methodology will also be used to examine the repeated load test data (Figs. 35 through 37).

Data from the repeated load tests can also be examined in other ways. To illustrate the variations in total, elastic, and permanent strain with load repetitions, data for the specimen whose permanent strain characteristics are shown in Fig. 37 are plotted in Fig. 38. The permanent strain per load application relationship shown in this figure was obtained by differentiating the curve of the form of equation (15) which has been fit to the data of Fig. 37. In Fig. 38 it will be noted that after about 100 stress repetitions, the permanent strain per cycle is quite small.

As noted earlier, an alternative solution to estimate rutting in asphalt concrete is to make use of a creep compliance, $\varepsilon(t)/\sigma_0$, for the asphalt bound material which can be used in turn in the VESYS II program developed by the FHWA. The equipment developed in this investigation can be adapted to such a test procedure. As with the repeated loading studies, at the time of this report only limited testing had been accomplished. Results of extention tests over a range in temperatures are shown in Fig. 39.

SUMMARY

During the year a number of facets of the pavement design process have been examined.

Results of the slab test study indicate, at least to a reasonable degree, that the results of laboratory determined fatigue characteristics can be used to predict the fatigue response of paving slabs subjected to repeated loading under controlled conditions. Moreover the results of this study lend additional support to the use of elastic theory to predict the response of asphalt-bound materials subjective to moving traffic provided the appropriate stiffnesses of such materials (as a function of loading time and temperature) are used.

With regard to loading times for determination of stiffnesses of asphalt mixtures, guidelines have been suggested herein based on the results of a number of investigations, including a detailed study as a part of this research program. Accordingly it is believed that sufficient information is now available to properly select the stiffness of an asphalt bound material in a pavement section for a particular vehicle speed and ambient temperature.

Preliminary studies indicate that the accumulation of permanent deformation in fine-grained soils with number of stress applications may be expressed by the relationship:

$$\varepsilon_1^p = A\ N^b$$

Such a relationship has the potential to assist in estimating the development of rutting with traffic in a pavement structure using elastic layer theory to estimate stresses and equation (12) presented herein, i.e.,

$$\delta_1^p\ (x,y) = \sum_{i=1}^{n} (\varepsilon_1^p \Delta z_1)$$

Estimation of the accumulation of permanent deformation in the asphalt portion of the pavement section appears to require a more detailed laboratory characterization procedure than that required for subgrade materials. The stress state, shape of the stress pulse, loading time and temperature all appear to be important variables in assessing this response. Some guidelines for loading conditions have been presented herein and will be used as the basis for research during this next year.

ACKNOWLEDGMENTS

The authors wish to acknowledge support provided this project by the Institute of Transportation and Traffic Engineering of the University of California in the form of shop, office and research facilities.

The contributions of Mr. Norio Ogawa, Research Assistant, and Dr. Charles Freeme on leave from the National Institute of Road Research, South Africa are gratefully acknowledged.

REFERENCES

1. Barksdale, R., "Compressive Stress Pulse Times in Flexible Pavements For Use in Dynamic Testing", Highway Research Record, No. 345, Highway Research Board, 1971.

2. Brown, S.F., "Determination of Young's Modulus for Bituminous Materials in Pavement Design", Highway Research Record, No. 431, Highway Research Board, 1973.

3. Finn, F.N., K. Nair, and C.L. Monismith, "Applications of Theory in the Design of Asphalt Pavements", Proceedings, Vol. 1, Third International Conference on the Structural Design of Asphalt Pavements, London, September 1972.

4. Hofstra, A. and C.P. Valkering, "The Modulus of Asphalt Layers at High Temperatures: Comparison of Laboratory Measurements Under Simulated Traffic Conditions with Theory", Proceedings, Vol. 1, Third International Conference on the Structural Design of Asphalt Pavements, London, September 1972.

5. Miura, Y., "A Study of Stress and Strain in the Asphalt Pavement of Tomei-Highway", Proceedings, Vol. 1, Third International Conference on the Structural Design of Asphalt Pavements, London, September 1972.

6. Thrower, E.N., N.W. Lister, and J.F. Potter, "Experimental and Theoretical Studies of Pavement Behaviour Under Vehicular Loading in Relation to Elastic Theory", Proceedings, Vol. 1, Third International Conference on the Structural Design of Asphalt Pavements, London, September 1972.

7. Witczak, M., "Design of Full-Depth Asphalt Airfield Pavements", Proceedings, Vol. 1, Third International Conference on the Structural Design of Asphalt Pavements, London, September 1972.

8. Pell, P.S., "Prepared discussion, Session IV", Third International Conference on the Structural Design of Asphalt Pavements, London, September 1972.

9. Verstraeten, J., "Moduli and Critical Strains in Repeated Bending of Bituminous Mixes - Application to Pavement Design", Proceedings, Vol. 1, Third International Conference on the Structural Design of Asphalt Pavements, London, September 1972.

10. Kirk, J.M., "Relations Between Mix Design and Fatigue Properties of Asphaltic Concrete", Proceedings, Vol. 1, Third International Conference on the Structural Design of Asphalt Pavements, London, September 1972.

11. Monismith, C.L., J.A. Epps, D.A. Kasianchuk, and D.B. McLean, Asphalt Mixture Behavior in Repeated Flexure, Report No. TE 70-5, University of California, Berkeley, Dec. 1970, 303 pp.

12. Barksdale, R.D., "Laboratory Evaluation of Rutting in Base Course Materials", Proceedings, Third International Conference on the Structural Design of Asphalt Pavements, 1972.

13. Romain, J.E., "Rut Depth Prediction in Asphalt Pavements", Proceedings, Third International Conference on the Structural Design of Asphalt Pavements, University of Michigan, 1972.

14. Freeme, C.R., "Prediction of Permanent Deformation in Flexible Pavements", Unpublished Report, University of California, Berkeley, 1973.

15. Monismith, C.L. and D.B. McLean, Design Considerations for Asphalt Pavements, Report No. TE 71-8, University of California, Berkeley, December 1971.

16. Majidzadeh, K., Analysis of Fatigue and Fracture of Bituminous Paving Mixtures, Columbus: Ohio State University Research Foundation, May 1970, (Final report of Project RF 2845, Phase 1).

17. Highway Research Board, "Structural Design of Asphalt Pavements to Prevent Fatigue Cracking", Special Report 140, 1973.

18. California Division of Highways, "Test Method No. 304", in Materials Manual, 1, 1963.

19. Secor, K., Viscoelastic Properties of Asphalt Paving Mixtures, Doctor of Engineering Dissertation, University of California, Berkeley, 1962.

20. Reissner, E., "Stresses in Elastic Plates Over Flexible Subgrades", Transactions, ASCE, 1957.

21. Warren, H. and W.L. Dieckmann, Numerical Computation of Stresses and Strains in a Multiple-Layer Asphalt Pavement System, Internal Report, Unpublished, Chevron Research Corporation, 1963.

22. Peutz, M.G.F., H.P.M. van Kempen, and A. Jones, "Layered Systems Under Normal Surface Loads", Highway Research Record, No. 228, Highway Research Board, Washingtin, D. C.: 1966.

23. Ahlborn, G. ELSYM5, Computer Program for Determining Stesses and Deformation in a Five Layer Elastic System, University of California, Berkeley.

24. McLean, D.B., Permanent Deformation Characteristics of Asphalt Concrete, Ph.D. Dissertation, University of California, 1973.

25. Seed, H.B. and J.W.N. Fead, "Apparatus for Repeated Loading Tests on Soils", In American Society for Testing and Materials, Papers on Soils - 1959 Annual Meeting, STP, No. 254, Phila: 1959, pp. 78-87.

26. Dehlen, G.L., The Effect of Non-Linear Material Response in the Behavior of Pavements Subjected to Traffic Loads, Ph.D. Dissertation, University of California, 1969.

27. Kenis, W.J. and T.F. McMahon, "Advance Notice of FHWA Pavement Design System and a Design Check Procedure", Prepared for Presentation at AASHO Design Committee Meeting, October 1972.

28. Mendelson, A., Plasticity: Theory and Application, MacMillan Company, New York, 1968.

TABLE 2 SLAB DATA

Slab No.	Mean height -in.	Ave Unit wt lb per cu ft	Ave void content* -percent
1	1.81	143.7	11.1
2	1.82	140.5	13.1
3	1.85	140.5	13.1
4	2.03	142.4	11.7
5	1.93	143.2	11.4
6	1.94	146.3	9.5
7	1.87	142.4	11.9
8	1.99	143.4	11.3
9	1.82	140.4	13.2
10	2.08	140.4	13.2
11	1.89	141.7	12.4
12	1.91	142.5	11.9

---

*Void content determined by weighing specimens coated with talc in air and in water.

TABLE 1 SUMMARY OF TIMES OF LOADING FOR DETERMINATION OF ASPHALT CONCRETE STIFFNESS

Type of Pavement	Investigator(s)	Vehicle Speed	Time of loading (or frequency)
Highway	Finn et al (3)	30-40 mph	0.015 sec.
	Hofstra and Valkering (4)	-	$\Delta t = 0.4 \times d$ where d = width of strain signal
	Miura (5)	40-80 kph	0.04 to 1.0 sec.
	Thrower et al (6)		length of stress pulse σ_z at top of subgrade* $f = \frac{1}{time}$
Airfields	Witczak (7)	10-20 mph	f = 2 cps.

* For very soft asphalt layers, Thrower suggests using the length of the pulse in the asphalt layer.

TABLE 3 SLAB TEST CONDITIONS

Slab No.	Testing temperature -°F	Subgrade reaction -pci	Applied stress -psi	Diameter of loading foot -in.
1	68	200	75 to 125	2
2	40	200	125 to 250	2
3	68	57	75	2
4	68	57	75	2
5	68	57	75	2
6	68	57	75	2
7	68	57	100	2
8	68	57	100	2
9	68	57	100	2
10	68	57	100	2
11	68	57	100	5
12	68	57	100	5

Table 4 Stiffness Data, Beam Specimens Obtained From Slab Specimens After Repeated Loading

		Stiffness*				Air Void Content - percent		
Slab No.	Temperature	Applied Stress - psi	Mean psi x 10^5	Std Dev. psi x 10^5	Correlation coefficient, C_v	Mean percent	Std Dev. percent	Correlation coefficient, C_v
1	68°F	100	1.92	0.25	13.2	10.8	0.8	7.8
2	40°F	150	5.88	0.50	8.5	14.7	0.3	1.8
3	68°F	75	1.52	0.11	7.5	11.8	0.2	1.7
4	68°F	75	1.48	0.24	16.5	13.4	0.4	2.7
5	68°F	75	2.27	0.49	21.4	11.3	0.8	7.4
6	68°F	75	2.62	0.42	16.0	9.8	0.3	2.8
7	68°F	100	1.73	0.10	6.0	12.2	0.2	1.9
8	68°F	100	1.62	0.15	9.2	14.5	0.3	2.1
9	68°F	100	1.83	0.12	6.7	11.6	0.1	0.4
10	68°F	100	1.95	0.20	10.4	13.3	0.5	3.6

*Measured at 0.1 sec. loading time and after conditioning of 200 stress applications.

TABLE 5 VALUES OF NUMBER OF LOAD APPLICATIONS (N_f) TO CAUSE FAILURE FOR EACH SLAB, 68°F (20°C).

Slab No.	Measured initial tensile strain in. per in x10^{-6}	"N_f" at which first break on crack sensor was recorded	"N_f" at which the relationships for deflection vs N_f and stiffness vs N_f deviates from straight line	"N_f" for flexural fatigue, beam specimen
1	150	400000[a]	More than one stress level was applied	700000
2	256	200000[a]	"	Tested at 40°F
3	313	9000[s]	37500 to 125000	72000
4	276	140000[a]	65000 to 165000	105000
5	200	249000[a]	150000 to 392000	298000
6*	150	17500[s] 692000[a]	125000 to 690000	700000
7	348	7200[s]	155000	50000
8*	405	8000[s] 50000[a]	50000	30000
9	385	140000[a]	145000	37000
10	285	12000	155000	90000

(a) Number of load applications which caused first break on aluminum foiltape.

(s) Number of load applications which caused first break on silver conductive paint.

(*) Slabs which were instrumented with aluminum foil tape for channels 1 to 8, and silver conductive paint for channels 9 to 16.

NOTE - Slabs No. 1, 2, 4, 5 and 9 were instrumented with aluminum foil tape and slabs No. 3, 7 and 10 were instrumented with silver conductive paint.

TABLE 6 - COMPARISON OF COMPUTED AND MEASURED DEFLECTIONS IN SLABS

Slab No.	Computed values - in. x 10^{-3} at radial distances, r - in.							Measured values[c] - in. x 10^{-3} at radial distances, r - in.				
	0[a]	1.0[a]	1.0[b]	2.5[b]	4.0[b]	6.0[b]	7.5[b]	0	2.5	4.0	6.0	7.5
1	5.6	5.4	5.9	5.0	4.2	3.2	2.5	6.8	6.0	-	4.5	4.0
2	8.7	8.6	8.6	8.0	7.2	6.0	5.1	11.3	10.0	8.5	8.0	5.3
3	10.7	10.5	11.6	10.7	9.6	8.0	6.8	13.0	13.0	11.5	10.0	7.5
4	9.2	9.1	10.2	9.6	8.6	7.3	6.3	10.5	10.5	10.0	9.0	7.0
5	6.9	6.8	8.9	8.4	7.7	6.6	5.8	10.3	10.2	10.0	9.0	5.5
6	6.5	6.3	8.3	7.8	7.2	6.2	5.5	9.5	9.0	8.5	7.5	6.5
7	12.2	12.0	14.4	13.3	12.0	10.1	8.7	17.0	13.5	12.5	-	9.5
8	12.0	11.7	13.4	12.6	11.4	9.5	8.4	16.0	16.0	13.5	11.0	10.0
9	13.3	13.0	14.5	13.5	12.2	10.2	8.7	15.5	14.0	12.0	11.0	10.0
10	10.2	10.0	11.5	10.9	9.9	8.6	7.5	13.5	13.5	13.0	11.5	10.0

a. Computed from equ. (9)

b. Computed from equ. (10)

c. At 1500 stress applications.

TABLE 7 SUMMARY OF STRESS-TIME CONDITIONS FOR ASPHALT CONCRETE SPECIMENS SUBJECTED TO REPEATED LOADING

location in section	stress direction	approximate shape of stress-time curve	ratio of time of loading in horizontal and vertical directions	ratio of vertical to horizontal stress
near surface	vertical	square	Fig. 33	less than 1 $< \frac{\sigma_v}{\sigma_h} <$ 5.0
	horizontal	triangle		
intermediate depth	vertical	triangle	Fig. 33	horizontal stresses may be zero, tensile or compressive
	horizontal	triangle		
bottom	vertical	triangle	1.0	Fig. 34
	horizontal	triangle		

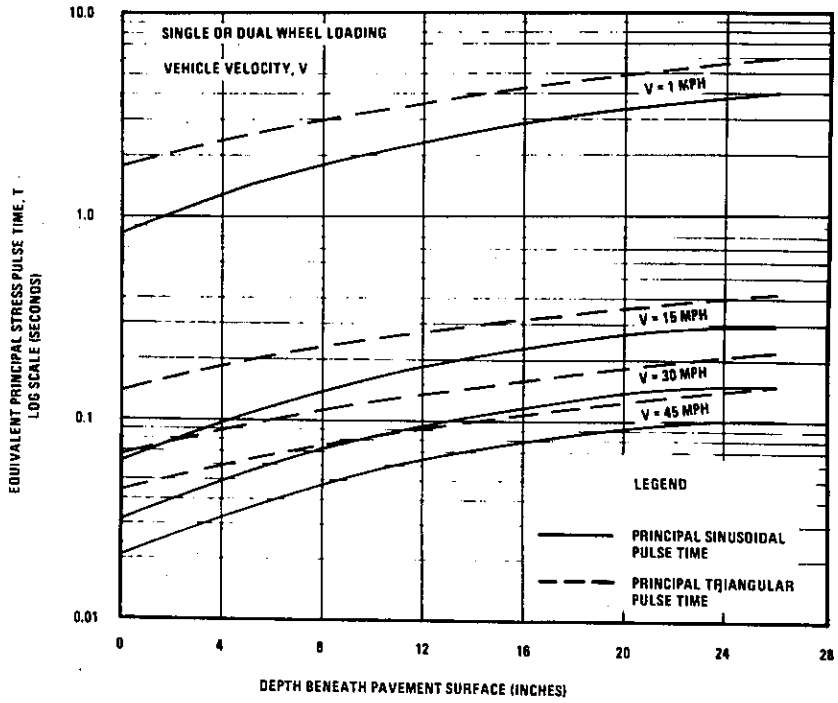

Fig. 1a – Variation of equivalent principal stress pulse time with vehicle velocity and depth. (After Barksdale)

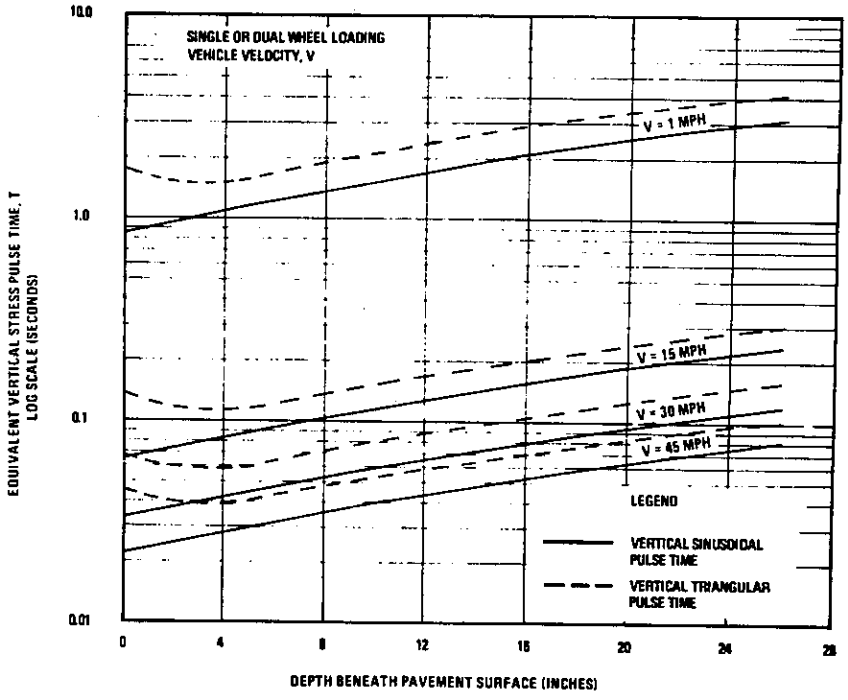

Fig. 1b – Variation of equivalent vertical stress pulse time with vehicle velocity and depth. (After Barksdale)

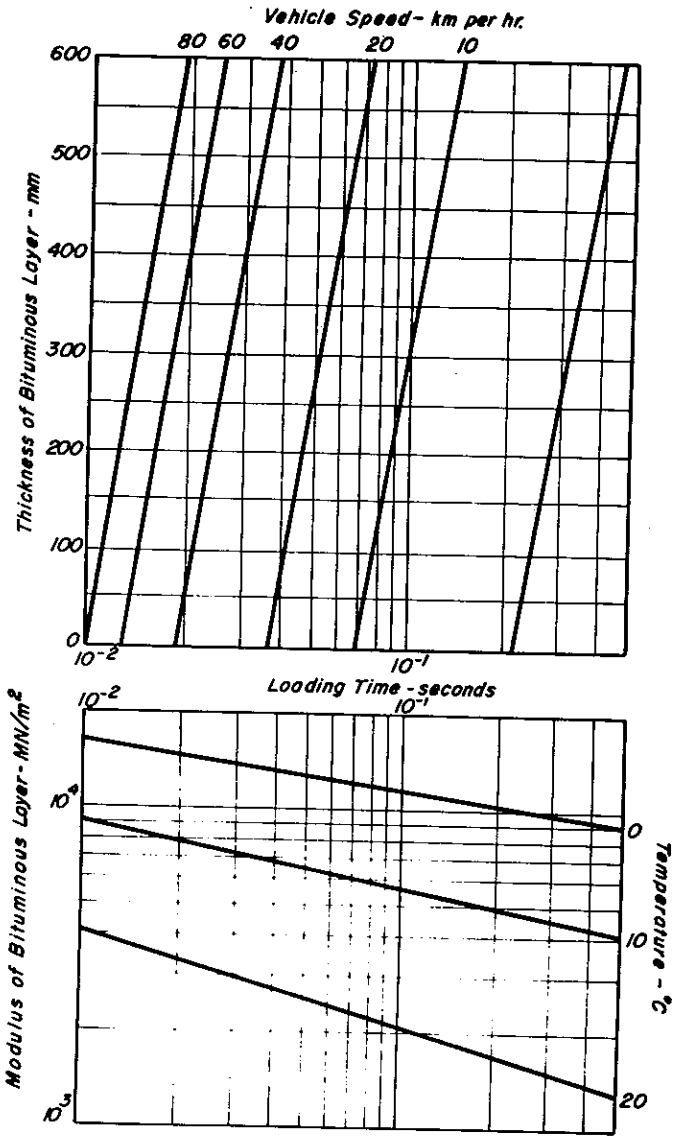

Fig. 2 — Stiffness of asphalt concrete. (After Brown)

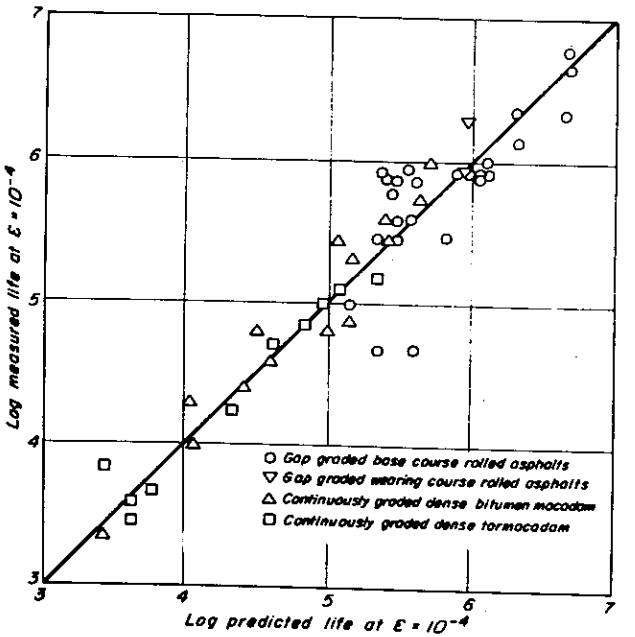

Fig. 3 — Relationship between predicted life using Equation (3) and measured life at a flexural strain $\epsilon = 10^{-4}$. (After Pell)

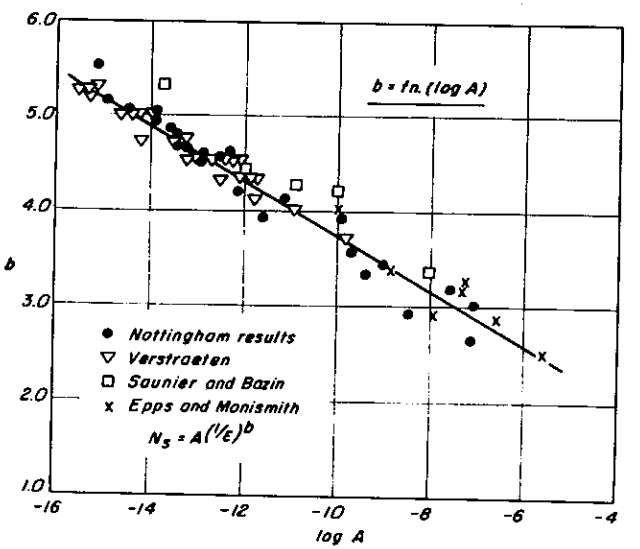

Fig. 4 — Relationship between m and log C in expression $N_f = C(1/\epsilon)^m$ for a series of mixes. (After Pell)

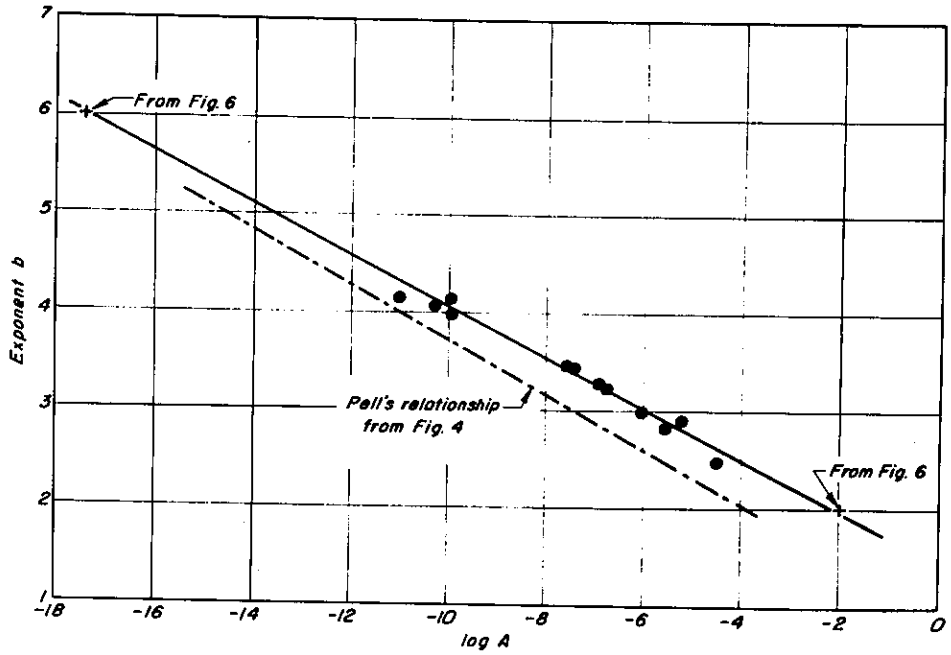

Fig. 5 — Relationship between log A and b in Equation $N_f = A(1/\epsilon)^b$.

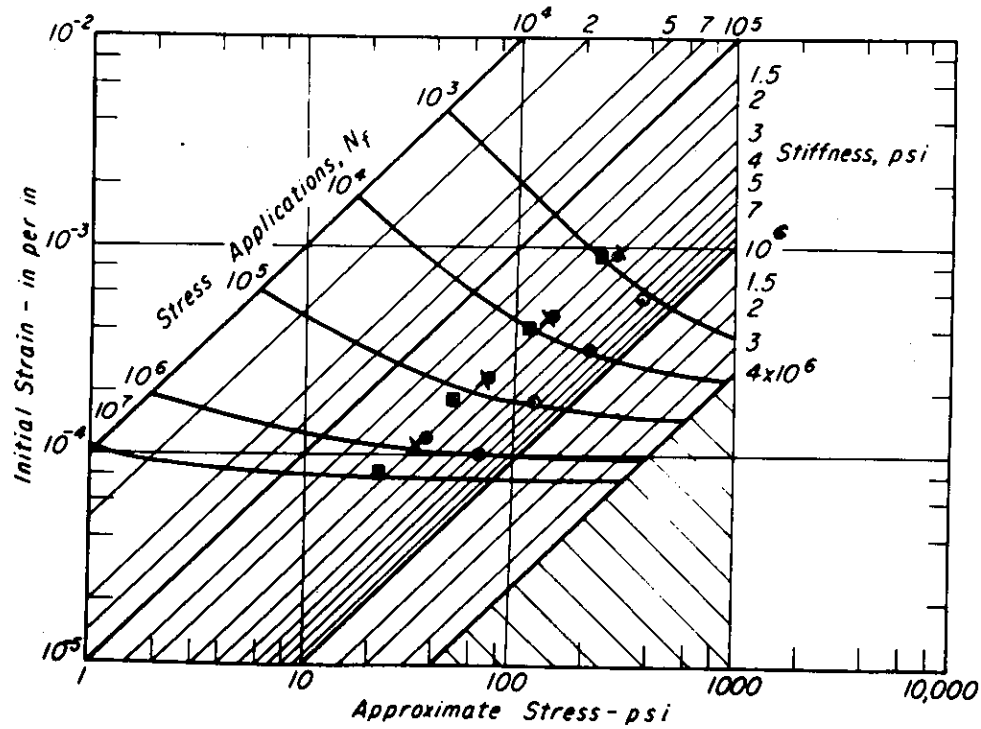

Fig. 6 – Relationship between stress, strain, stiffness, and fatigue life, California type mixtures, approximate void content — 5 percent.

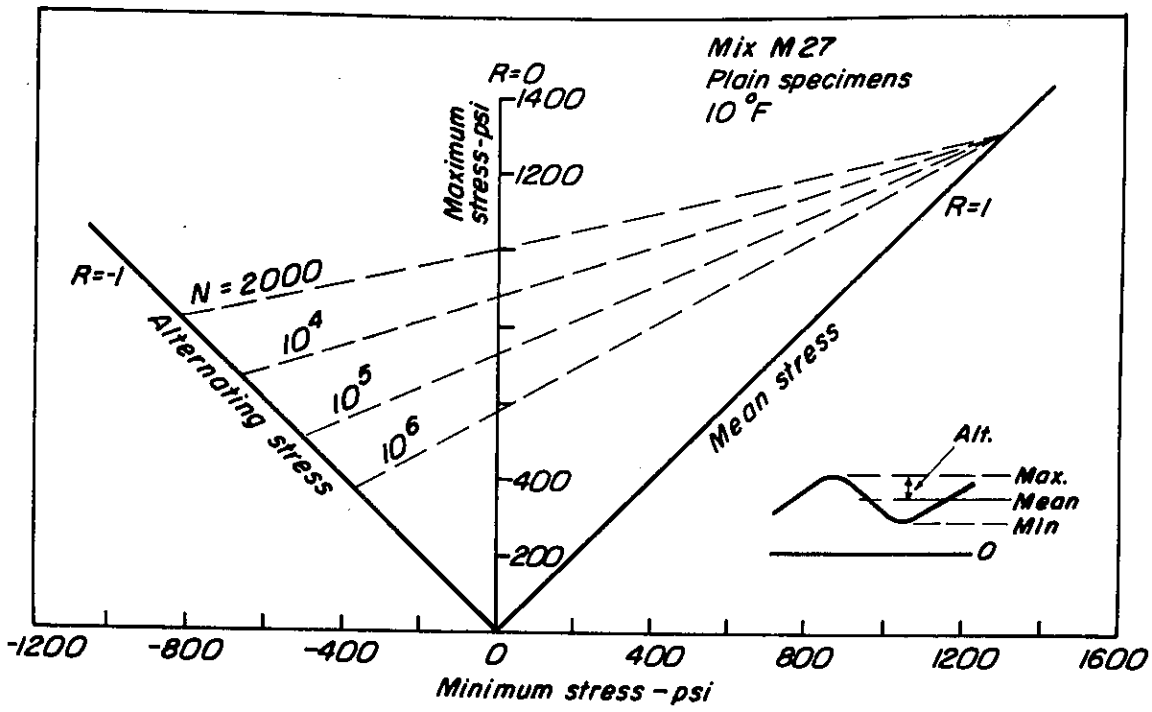

Fig. 7 – General representation of fatigue life on modified Goodman Diagram — Mix M27, 10°F.

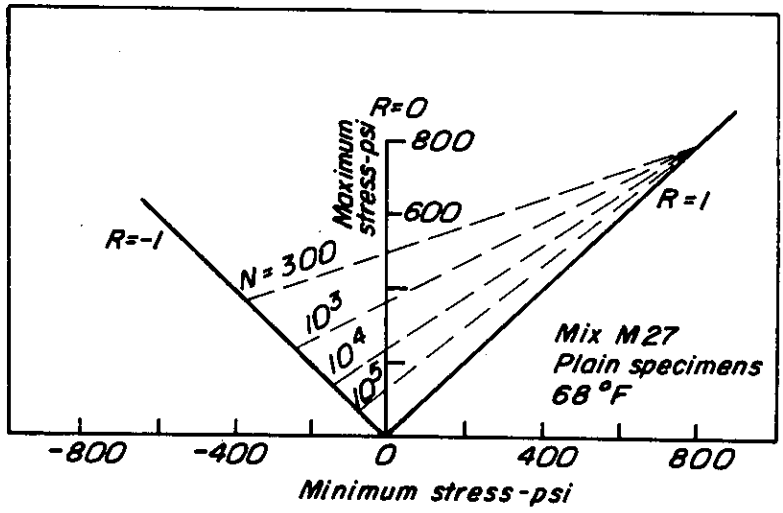

Fig. 8 – Representation of fatigue life on modified Goodman Diagram — Mix M27, 68°F.

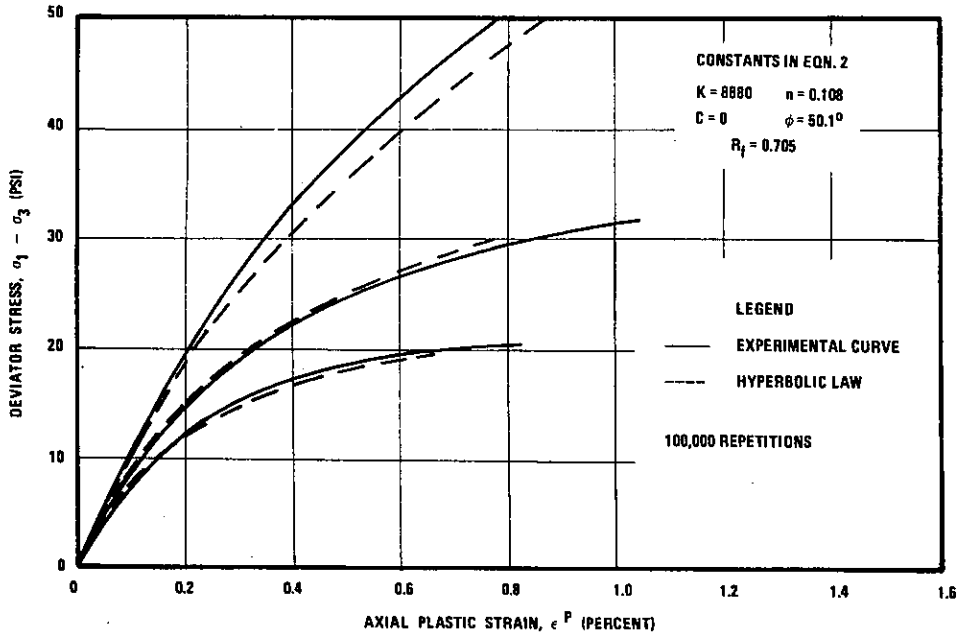

Fig. 9 – Comparison of calculated hyperbolic plastic stress-strain with experimental curves for a 21-79 soil aggregate-base 5. (After Barksdale)

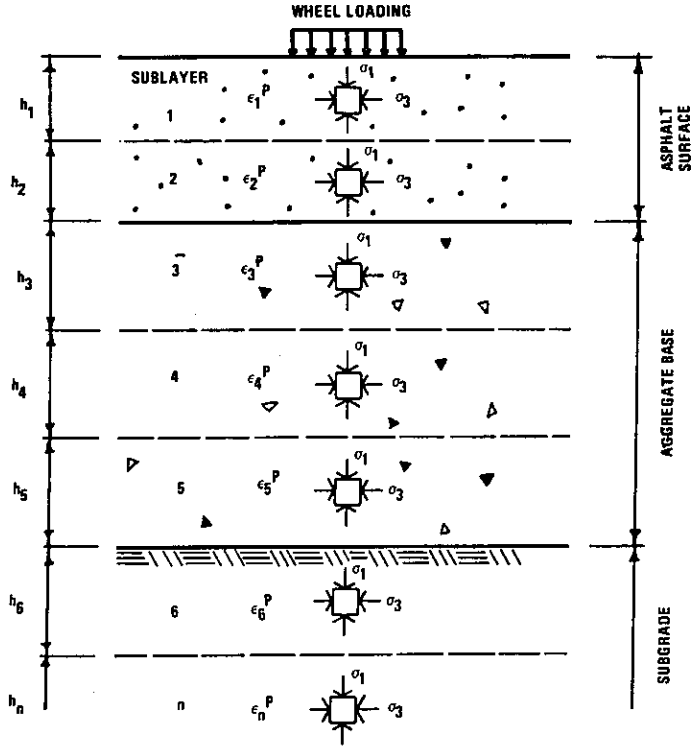

Fig. 10 – Idealization of layered pavement structure for calculating rut depth. (After Barksdale)

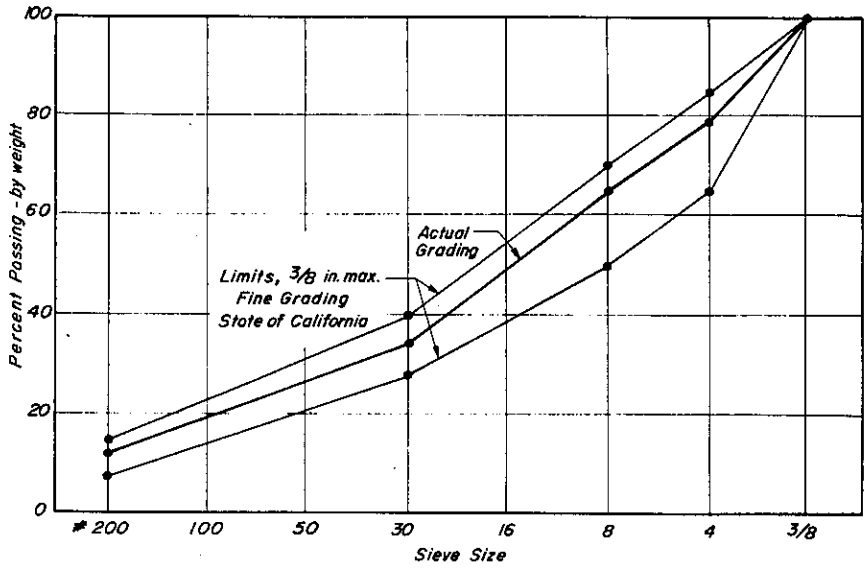

Fig. 11 — Aggregate gradation — slab specimens.

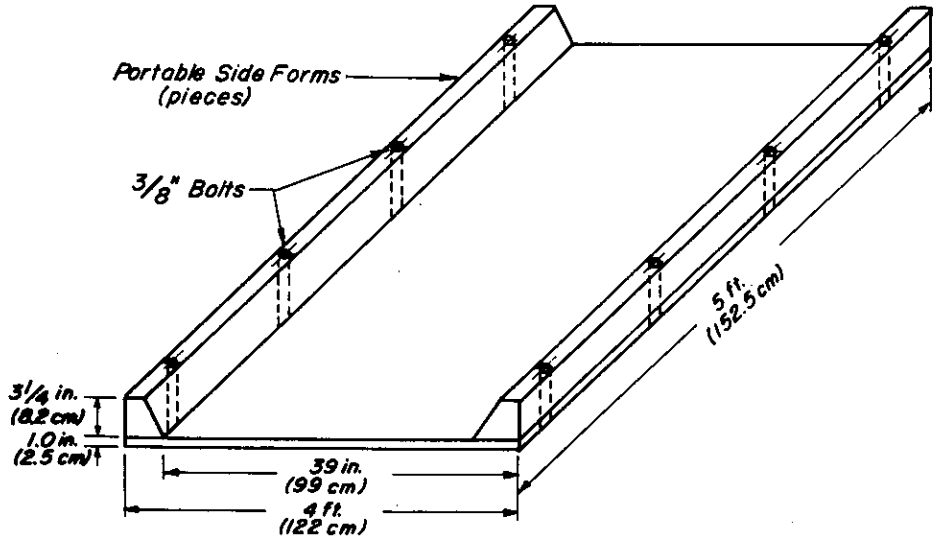

Fig. 12 — Form used to prepare slab test specimens.

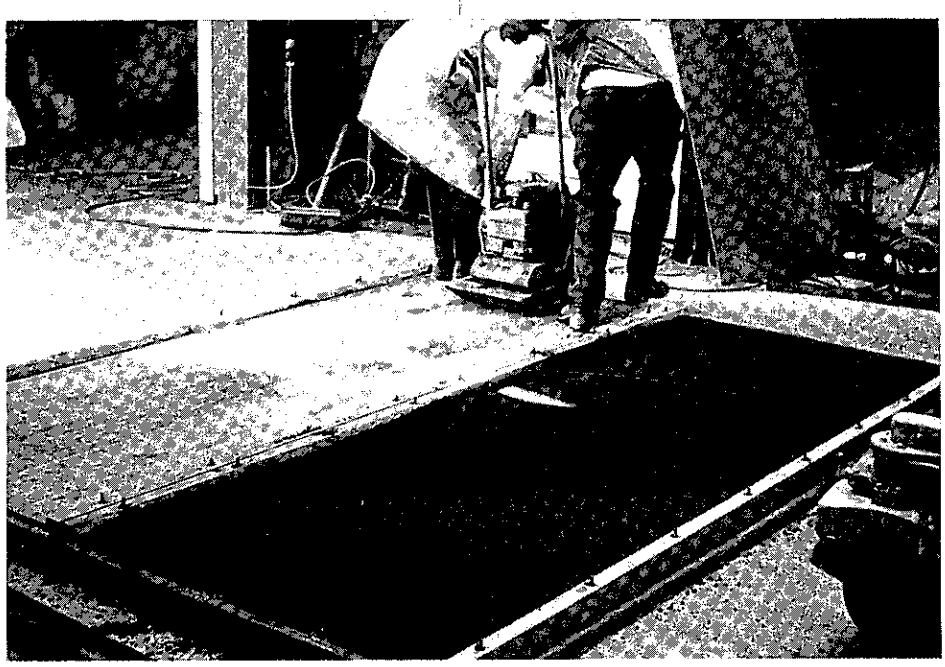

a. Compaction

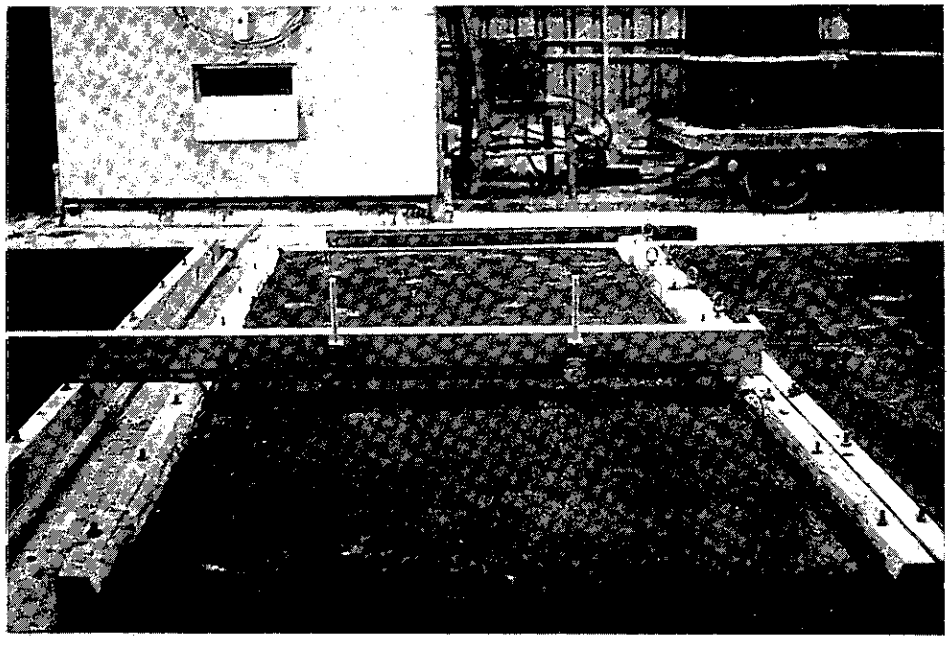

b. Thickness measurement for control of specimen height and density.

Fig. 13 – Preparation of slab specimens.

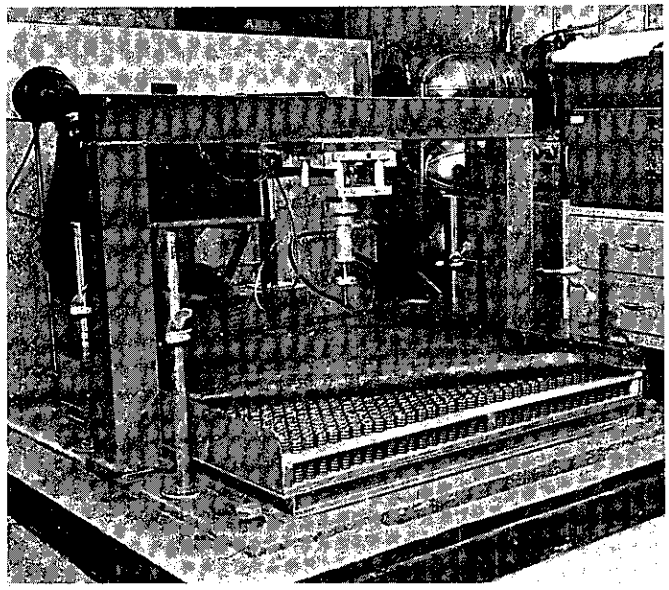

Fig. 14 — Slab testing device with rubber membrane stripped back to show spring base.

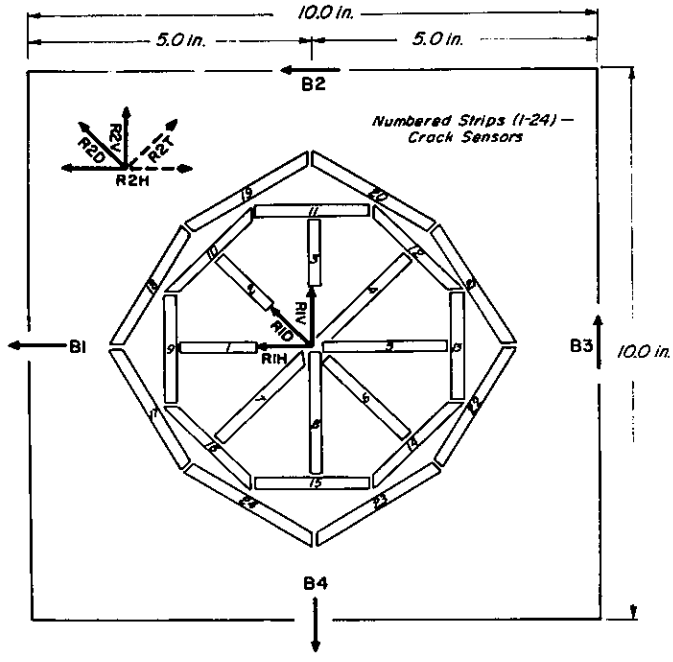

B1, B2, B3, B4 1 in. Single strain gages located at 5.0 in. from center of loading

R1H, R1V, R1D 3/4 in. Rosette strain gages located under loading foot

R2H, R2V, R2D or R2T 3/4 in. Rosette strain gages located at 5.0 in. from center of loading

Fig. 15 – Location of strain gages and crack sensors on the bottom surface of asphalt concrete slabs.

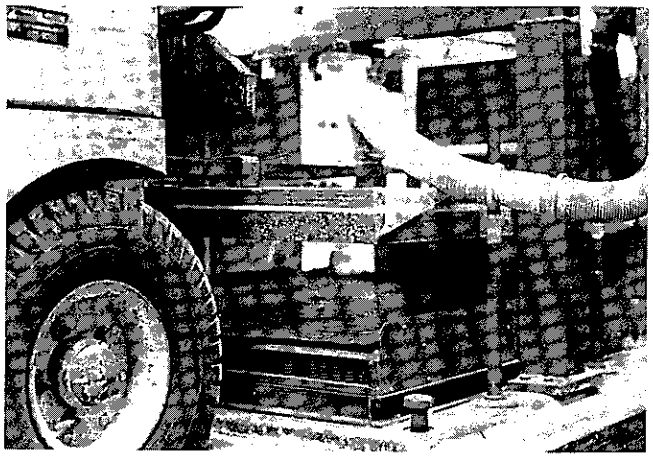

a.

b.

Fig. 16 — Slab being placed in slab testing device.

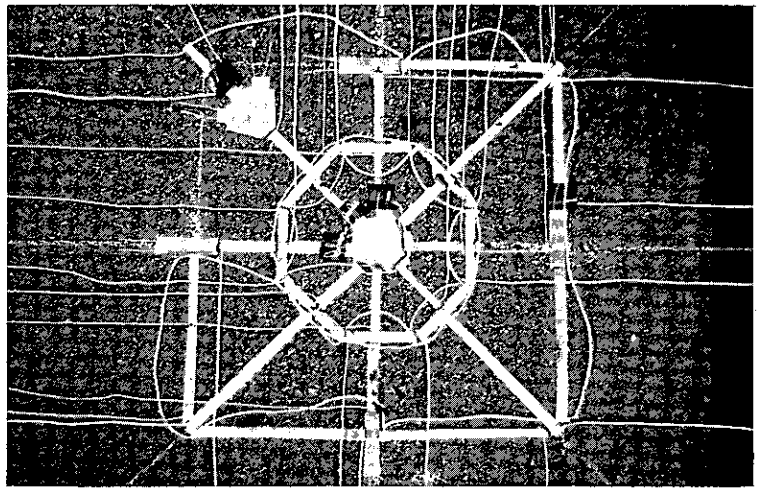

Fig. 17 — Bottom side of slab showing location and pattern of strain gages and aluminum foil tape crack sensors.

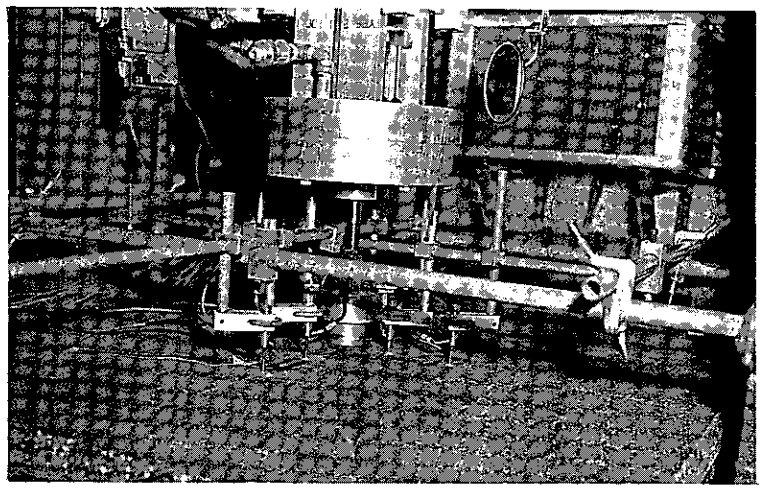

Fig. 18 — View of slab installed in slab testing device prior to start of testing.

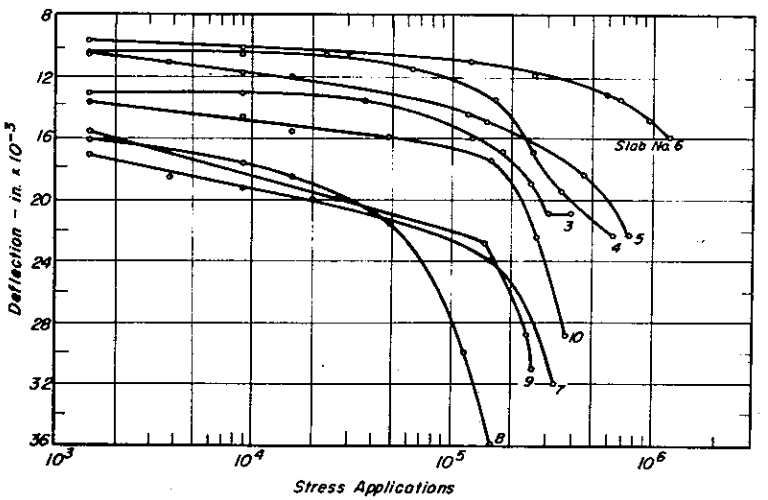

Fig. 19 – Measured deflection vs. stress applications at 68° F; slabs 3-6, 75 psi stress; slabs 8-10, 100 psi stress.

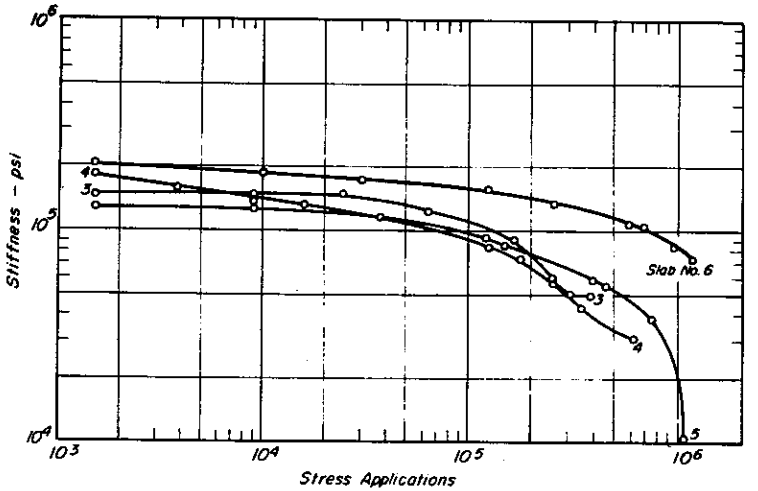

Fig. 20 – Computed stiffness vs. stress applications at 68° F; applied stress – 75 psi, $\nu = 0.5$.

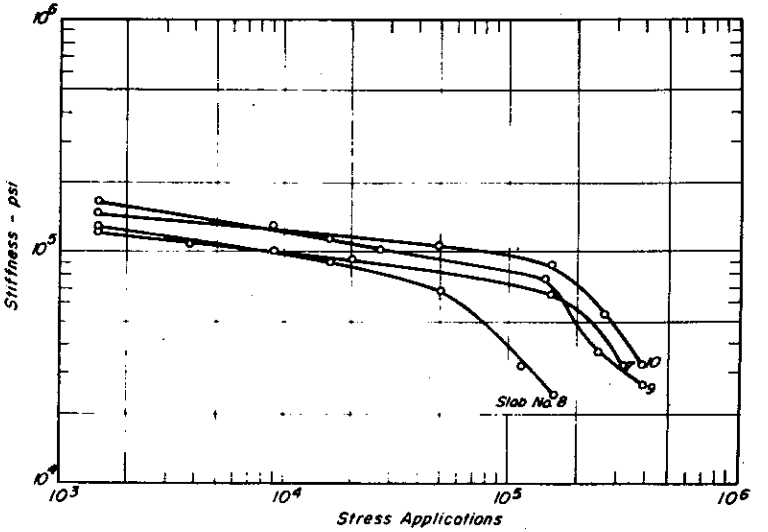

Fig. 21 – Computed stiffness vs. stress applications at 68° F; applied stress – 100 psi, $\nu = 0.5$.

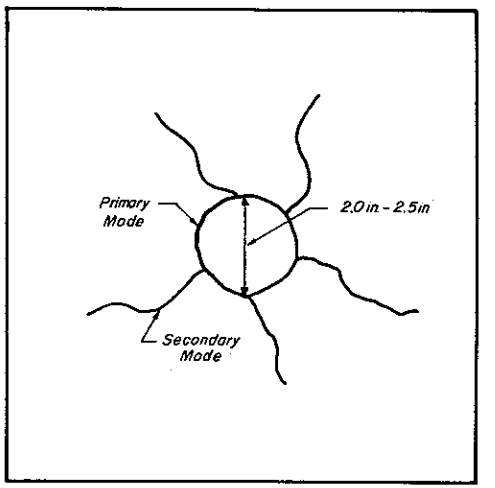

Fig. 22 – Final crack pattern.

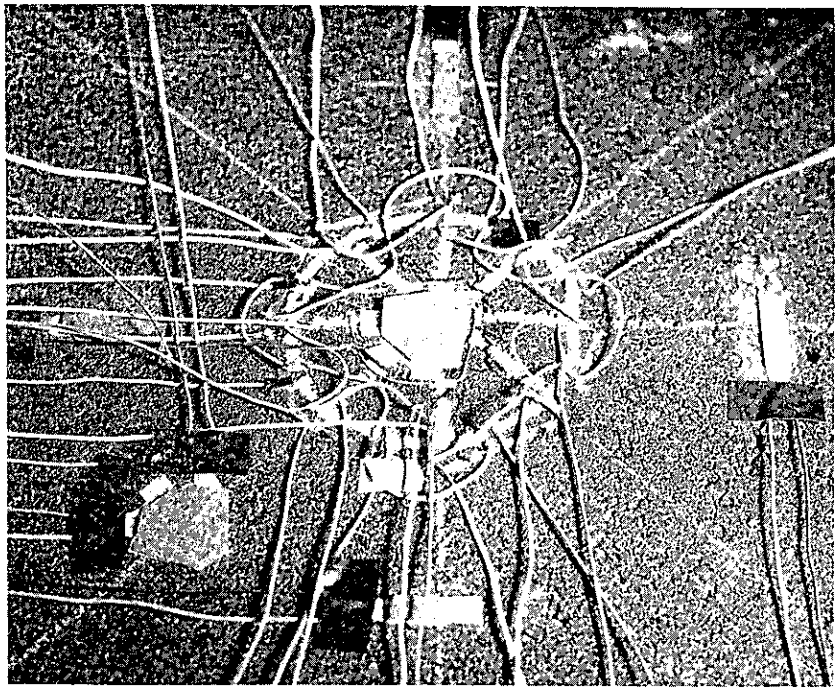

Fig. 23 – Crack pattern at base of slab, 75 psi, 2.0 in. diameter loaded area, 10^6 repetitions. (Note use of silver conductive paint as crack sensors.)

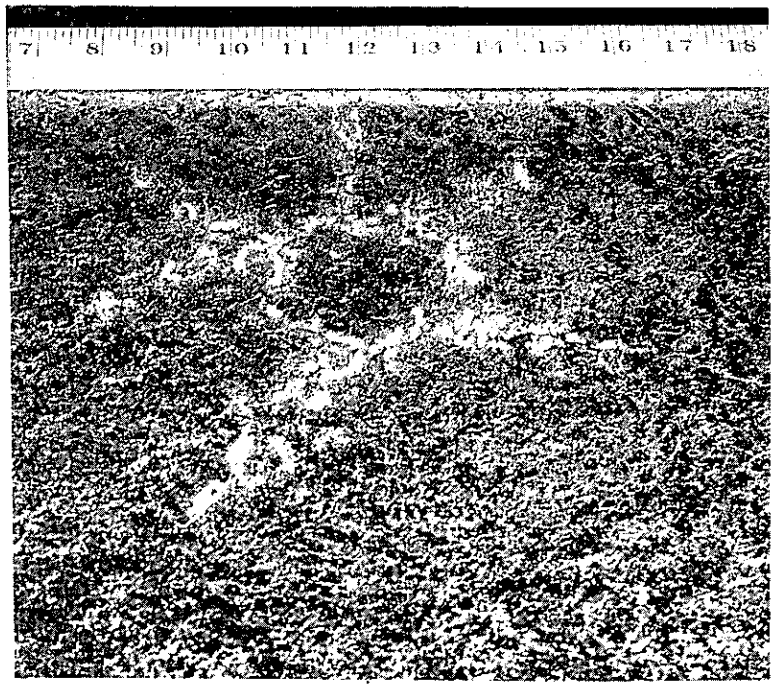

Fig. 24 – Crack pattern at base of slab, 100 psi, 5.0 in. diameter loaded area, 350,000 repetitions.

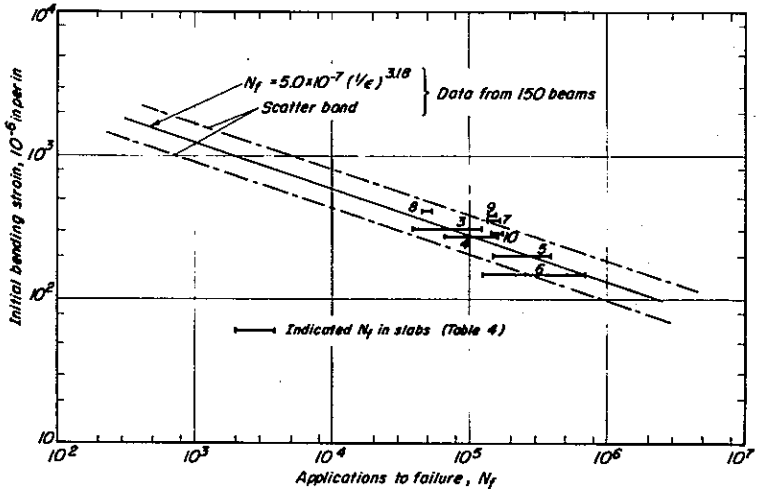

Fig. 25 – Comparison of service lives obtained from beam and slab specimens.

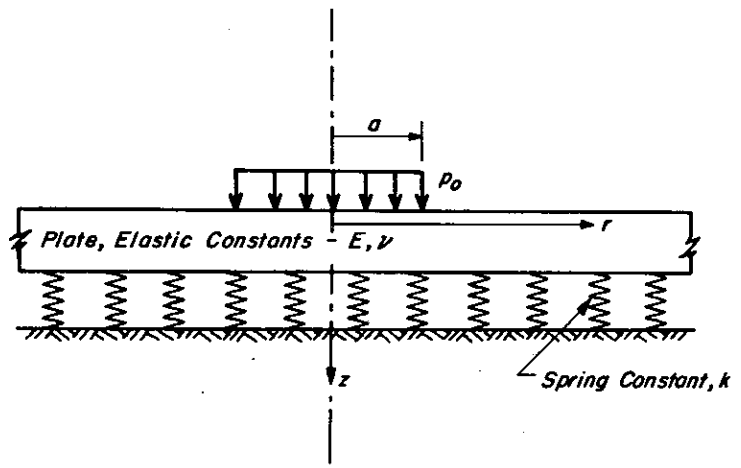

Fig. 26 – Schematic representation of plate on dense liquid subgrade.

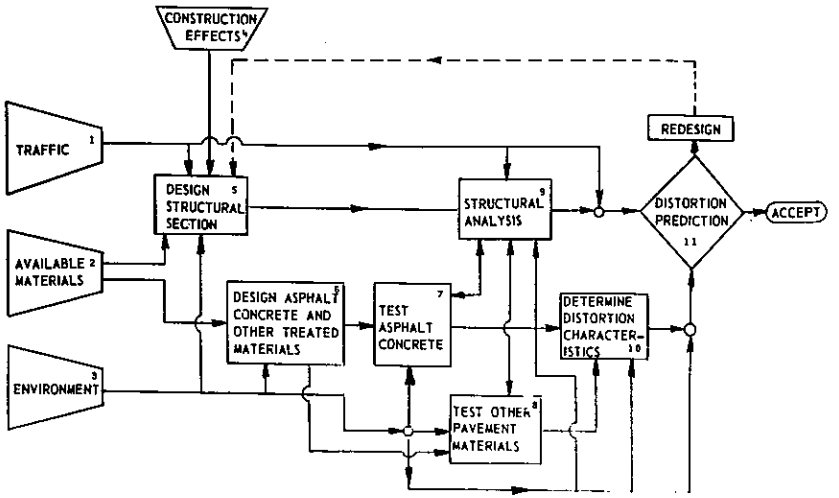

Fig. 27 – Block diagram of a distortion subsystem.

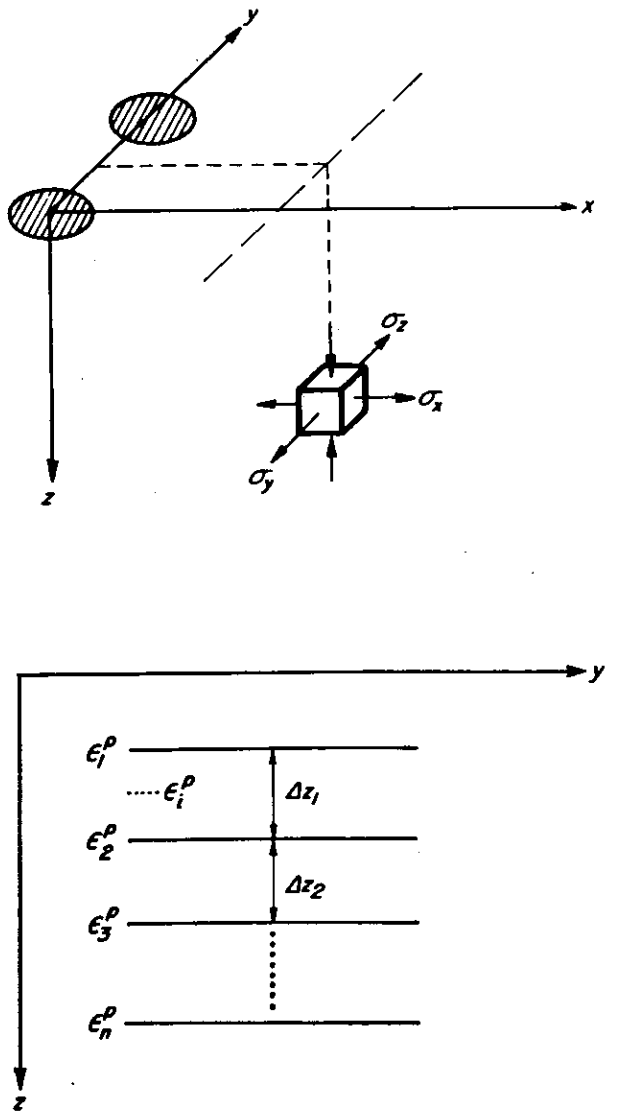

Fig. 28 – Schematic representation of pavement system used to estimate permanent deformation.

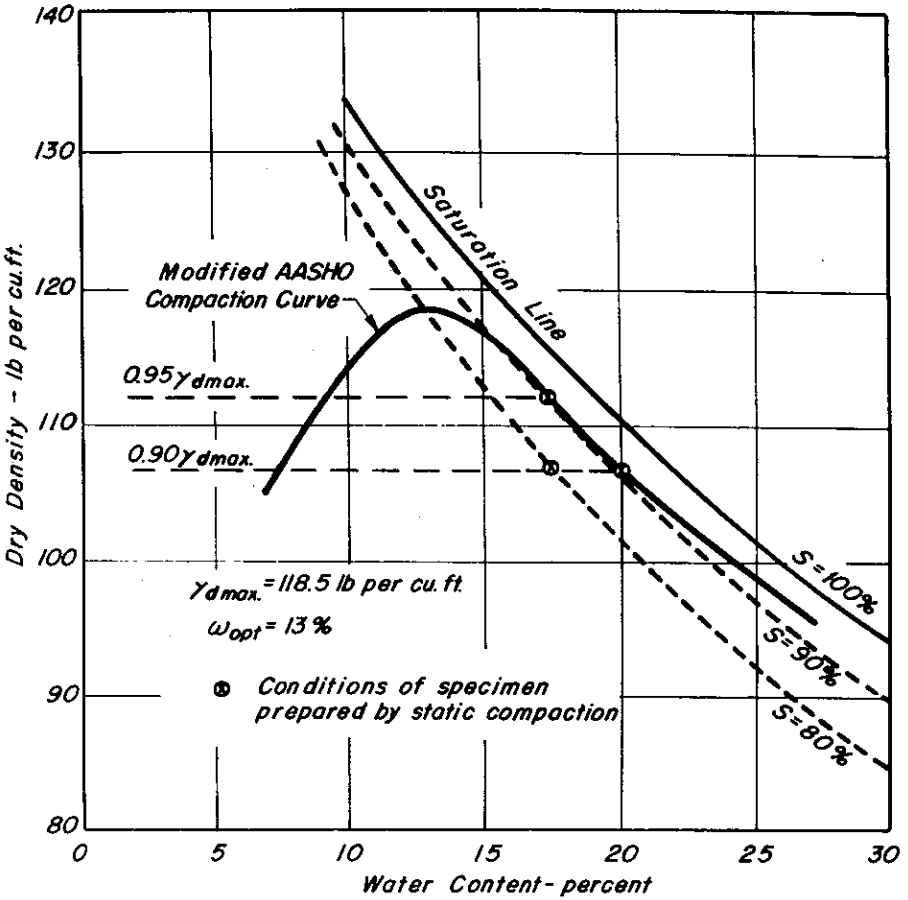

Fig. 29 – Density vs. water content relationship for Ygnacio Valley subgrade soil.

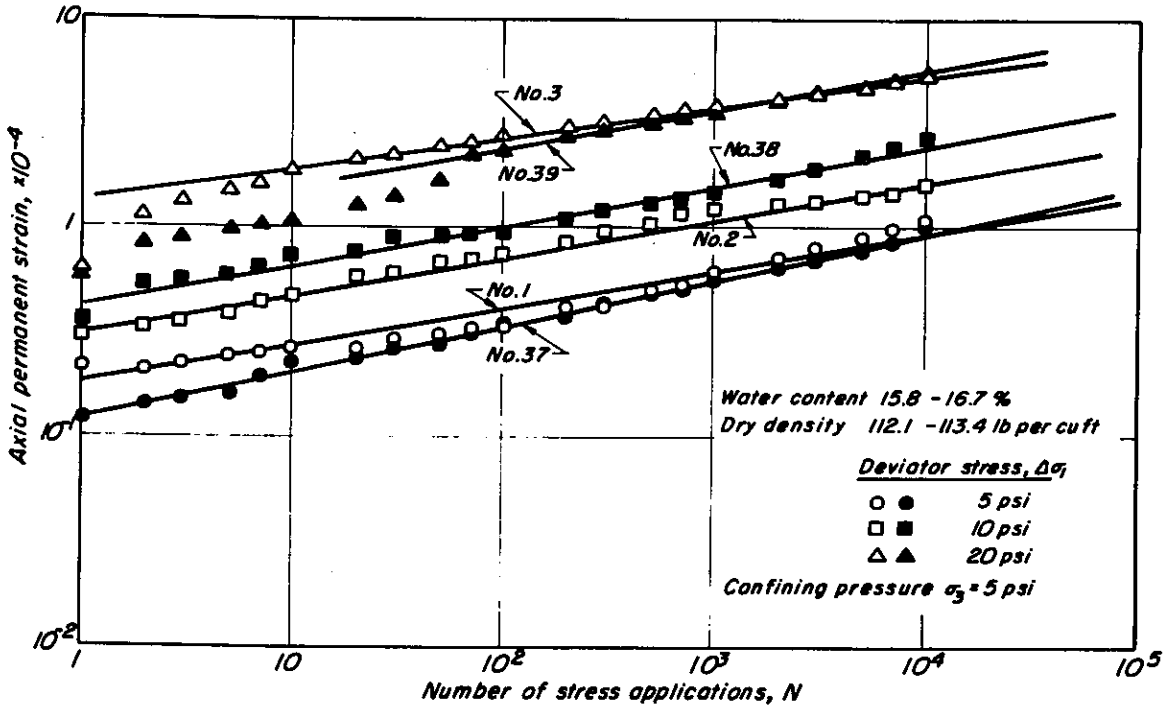

Fig. 30 – Axial permanent strain vs number of stress applications, Ygnacio Valley subgrade soil.

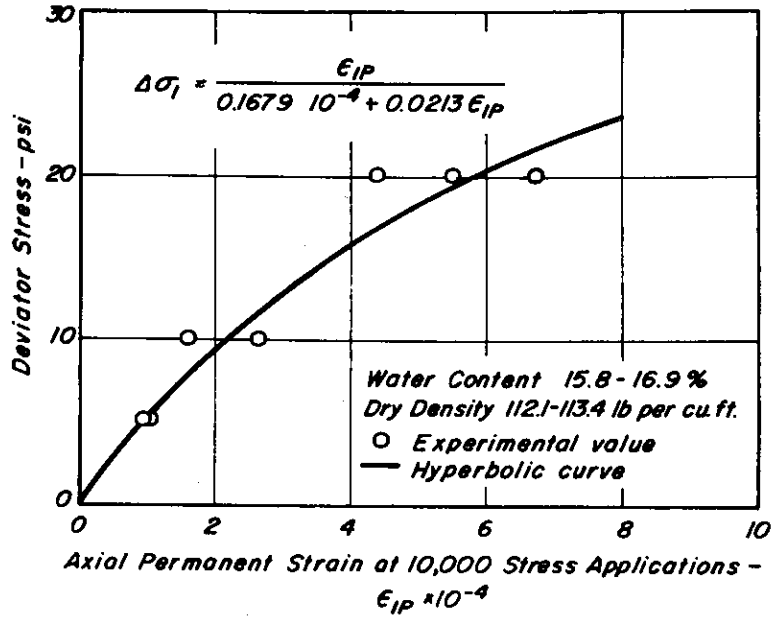

Fig. 31 – Relationship between deviator stress and permanent strain, N = 10^4 repetitions; Ygnacio Valley subgrade.

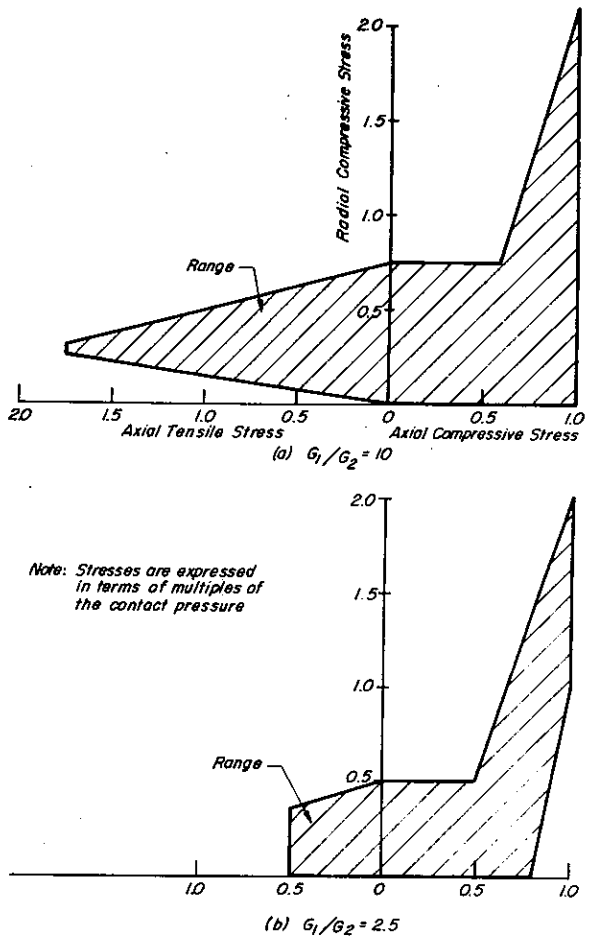

Fig. 32 – Probable ranges of stress combinations in asphalt layer (Layer 1) of a two layer system.

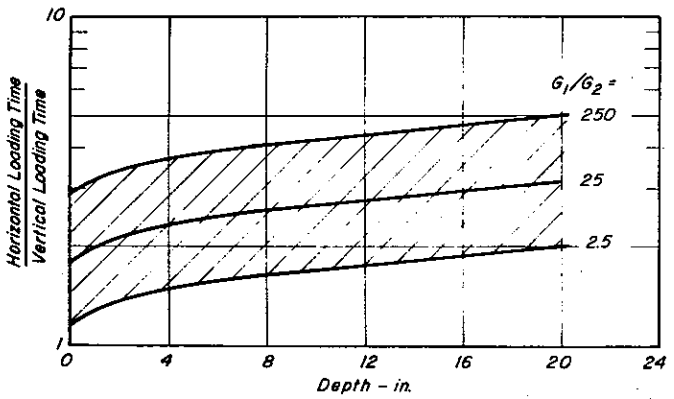

Fig. 33 – Ratio of horizontal stress loading time to vertical compressive stress loading time for range in modular ratios.

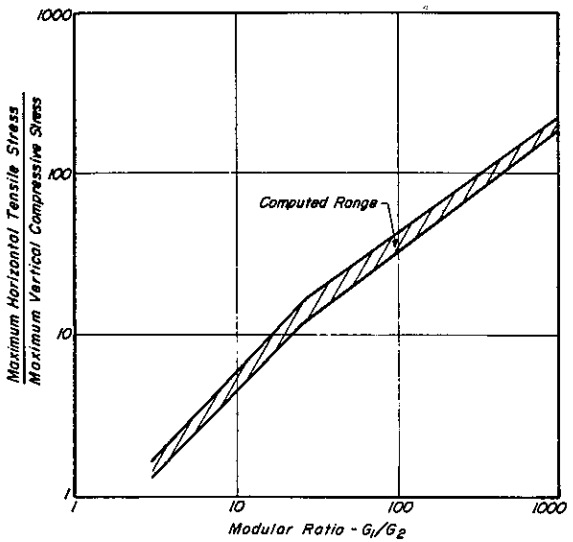

Fig. 34 – Ratio of the maximum horizontal tensile stress to the maximum compressive stress at the base of layer 1 vs modular ratio of the two layers.

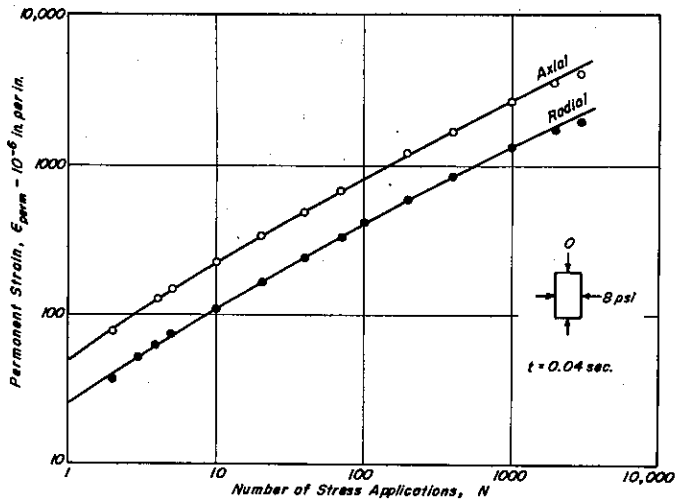

Fig. 35 — Relationships between permanent strain and stress applications, extension test — 67° F.

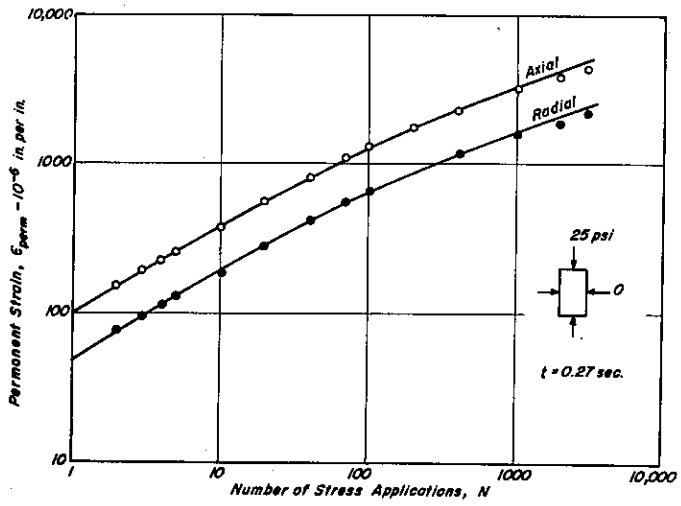

Fig. 36 — Relationships between permanent strain and stress applications, compression test — 85° F.

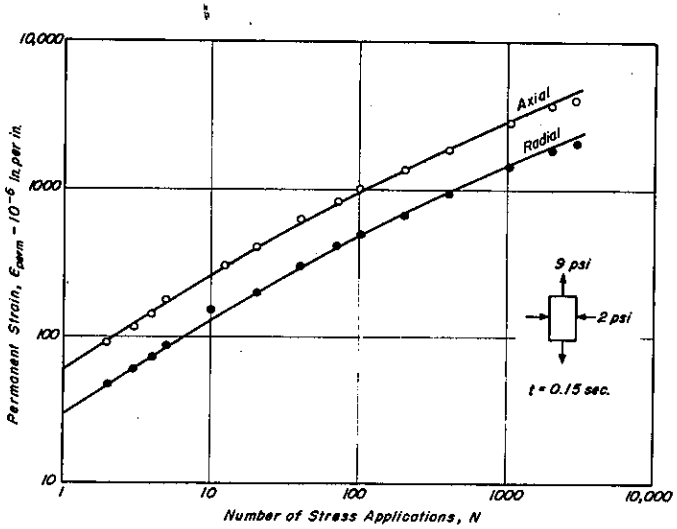

Fig. 37 — Relationships between permanent strain and stress applications, tension test — 100° F.

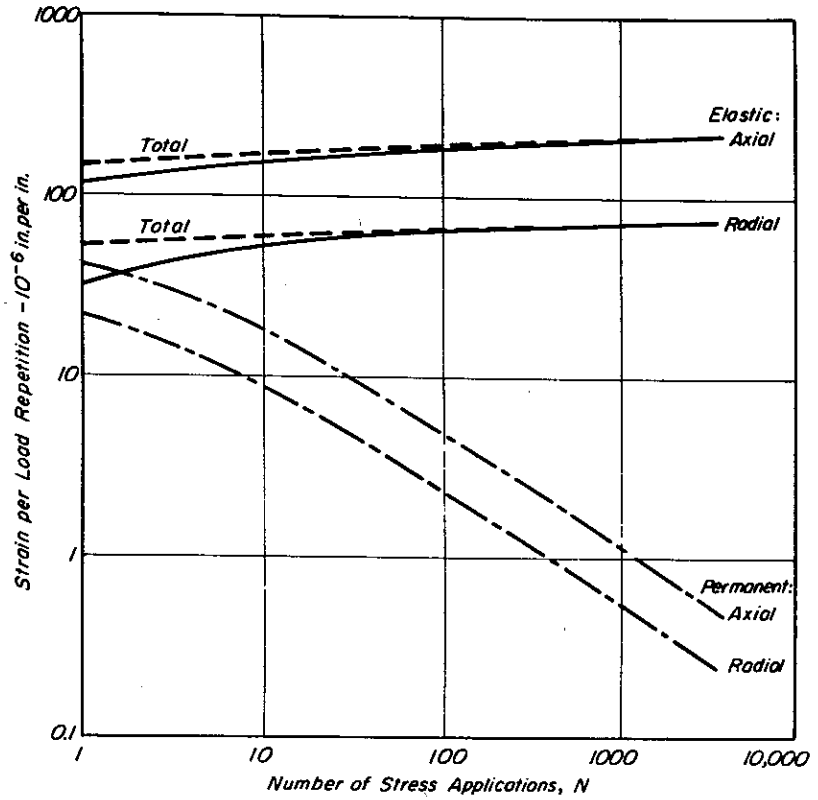

Fig. 38 – Strain per stress application relationships, tension test at 100° F (test conditions those of Fig. 37).

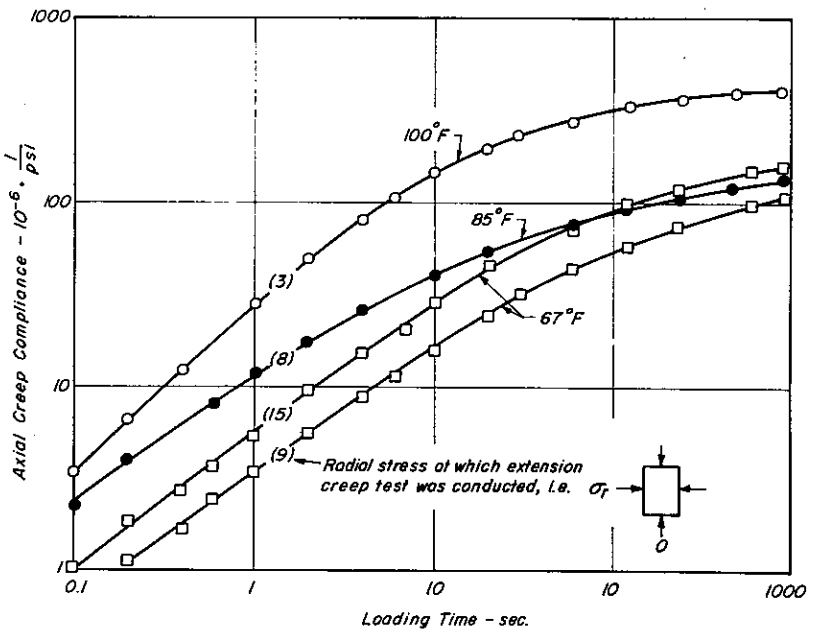

Fig. 39 – Axial creep compliance determined from extension tests over a range in temperatures.

APPENDIX A

TRIAXIAL COMPRESSION TEST TO MEASURE PERMANENT DEFORMATION OF SUBGRADE SOILS IN REPEATED LOADING: EQUIPMENT AND PROCEDURES

Repeated-load triaxial compression tests similar to those used for determination of resilient moduli were used to measure the accumulation of permanent deformation in subgrade soil specimens. The triaxial cell, shown schematically in Fig. A-1, can accommodate specimens 2.8 in. in diameter by 6 in. high.

Air was used for the confining pressure and only one level, 5 psi, was used.

Repeated loads were applied pneumatically at a load duration of 0.1 sec. and a frequency of 20 repetitions per minute.

Both axial and radial deformations were measured by LVDT's attached to the soil specimen as shown in Fig. A-1. Details of the clamps are shown in Figs. A-2a and A-2b.

The axial strain device measured the accumulation of permanent deformation over the center 3 in. of the specimens.

Measurement of the accumulation of permanent radial strain presented some difficulties initially because of soil creep at the clamps. To overcome this, the strain unit is suspended from springs as shown in Fig. A-1 and bonded to the membrane using an epoxy resin.

Repeated loads were applied over a range in axial stresses and as many as 100,000 stress repetitions were applied to an individual specimen.

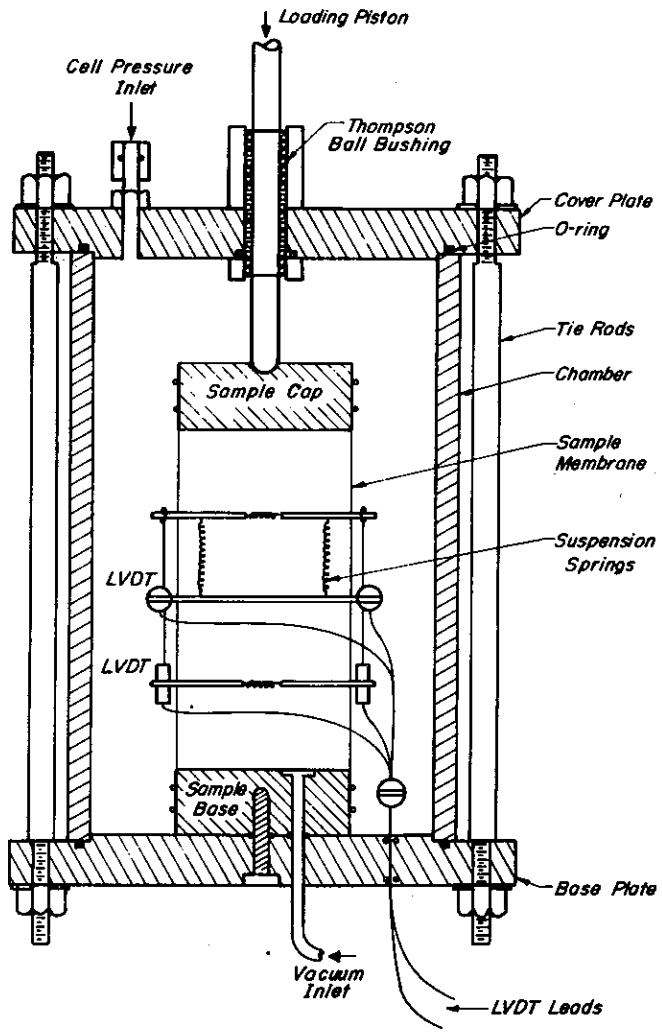

Fig. A-1 – Apparatus for repeated load test of soil.

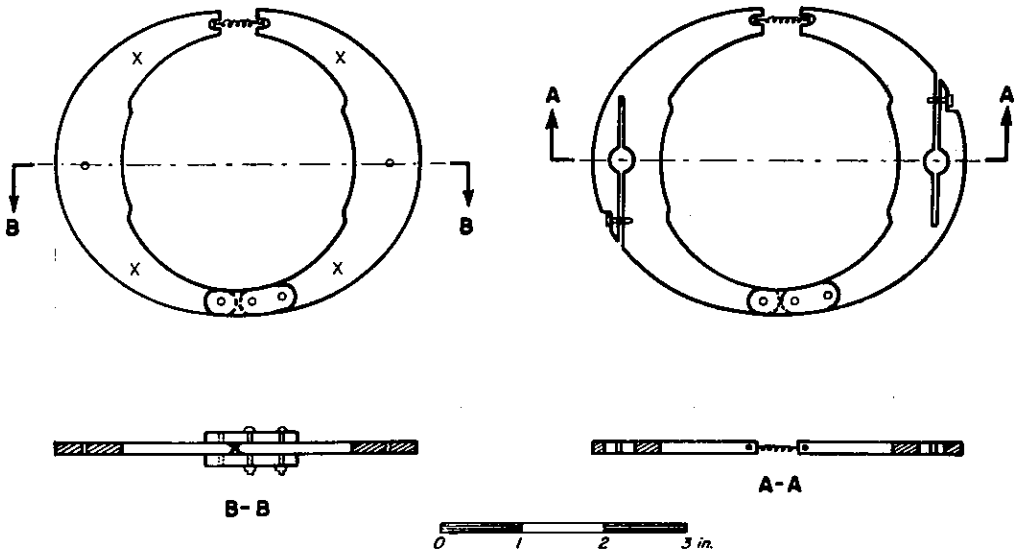

Fig. A-2a — LVDT clamps for axial strain measurement.

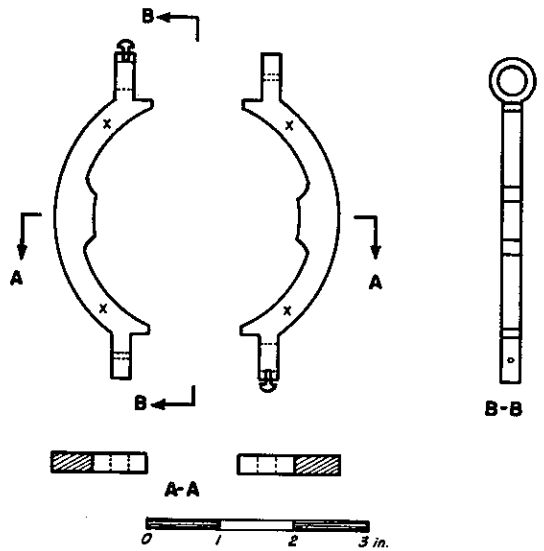

Fig. A-2b – LVDT clamps for radial strain measurement.

APPENDIX B

TRIAXIAL COMPRESSION TEST TO MEASURE PERMANENT DEFORMATION OF ASPHALT MIXTURES IN REPEATED LOADING: EQUIPMENT AND PROCEDURES

Equipment and Instrumentation

The triaxial compression test system used in this phase of the investigation was developed by Dehlen (26). In this system the axial and radial stresses can be independently applied, Fig. B-1. As seen in this figure, this independence is obtained by loading the specimen axially from the bottom with a loading area equal to that of the specimen; a Bellofram is used to seal the axial loading piston. Axial compression or tension is applied by use of a double acting 4 in. diameter Bellofram piston. Radial pressure is obtained by filling the chamber with silicone oil and applying air pressure to it through a Bellofram piston interface.

A pneumatic timer control unit was developed for the system consisting of four pneumatic timer elements and functioning as shown schematically in Fig. B-2. Two elements are activated at the start of the cycle and provide signals of duration t_1 and t_2. Signal t_1 represents the 'on-time' signal to either the axial or radial loading system while t_2 introduces a delay time prior to the activation of a third element. This element provides an 'on' signal of duration t_3 to the second loading element. The fourth timer controls the off-load of the system. Times t_1 to t_4 are adjustable from essentially zero to approximately 30 seconds.

Output signals from the timer involve only a small line flow of air, insufficient to operate large air valves. Therefore a booster system was required as shown in Fig. B-3. Using this approach and maintaining short flow distances from air reservoirs to the loading pistons, rise times (time from zero to full load) could be reduced to 0.007 seconds. Where longer load rise times were required, needle valves were introduced to the system to control the air flow rates. Due to limitations imposed by valve response times, the minimum load duration which could be obtained was 0.035 sec.

This equipment was also used for creep tests. For these tests the timer portion of the repetitive loading system was replaced by a digital clock reading to 0.01 min. The main air valves were operated using electric solenoid valves. A main switch activated the solenoid valves and timer simultaneously. System components are shown schematically in Fig. B-4. Use of high air pilot pressures resulted in rapid valve response times with the result that load rise times were less than 0.01 sec. in all tests. Loading times less than one minute were measured using the timer portion of the Sanborn recorder system while times greater than one minute were established from the digital clock.

Deformations in the specimens were measured using linear variable differential transformers (LVDT's) firmly attached to the specimens as shown in Fig. B-5.

Specimen Preparation

Asphalt concrete specimens were compacted at 230°F using a Triaxial Institute (or California) Kneading Compactor. During the compaction process, material was supplied continuously to the sample mold. This procedure reduces density variations which occur in specimens compacted in lifts and eliminates weaknesses which may occur at compaction interfaces. Compacted specimens were approximately 4 in. in diameter by 9 in. in height. Poorly compacted material at the top and base of the sample was removed by trimming each specimen to a height of approximately 8 in. The compaction schedule (number of tamps and tamping pressure) was evolved by a trial and error procedure. The procedure was varied until the range of variation of bulk specific gravity within a specimen was consistently less than 0.02. (NOTE: This variation was measured by sawing specimen into four discs, each about 2 in. high, and measuring the bulk specific gravity of each disc.)

Test Procedures

Prior to repeated load or creep tests all specimens were bonded to aluminum end caps using an epoxy adhesive. To insure proper axial alignment and parallelism of the caps a jig was used.

Special precautions were required to preclude leakage of the cell fluid through the membrane into the specimen. End caps were cleaned and polished prior to reuse thus ensuring a tight seal between the caps and the membranes. Leakage around the LVDT mounts was prevented

by use of a double membrane. Epoxy was used to attach the inner membrane to the specimen in the vicinity of the LVDT connection. A second membrane was then placed over the first. Leakage through the outer membrane was controlled by placement of a special sealant between the LVDT mounting block and the membrane.

Repeated Loading. While many different loading conditions exist in the pavement structure, only three have been chosen for study in the laboratory in part because of limitations of the pneumatic loading equipment to completely simulate the actual conditions. The conditions planned for study include:

(1) midway between the loaded areas, horizontal compression (extension tests)

(2) near the point of zero horizontal stress (unconfined compression tests)

(3) at the base of the layer, axial tension and radial compression, both having the same loading time (tension tests)

Due to the time dependent recovery properties of asphalt concrete, the amount of permanent deformation measured would be expected to depend on the time interval between load applications. Initially the off-load time will not be considered as a variable. In preliminary tests it was observed that deformation recovery approached zero at a cycle time of 6 seconds, Fig. B-6. This value was selected for use in the study.

Creep Loading

Prior conditioning influences the response of asphalt concrete in creep loading. In this study the procedure which has finally been adopted includes the application of a stress of larger magnitude than than to be used in test for a period of 10 min. followed by two repetitions of the desired stress applied for a period of 15 min. Recovery times of 1 to 1.5 hours are allowed between each load application. Deformations from the second or third application are used for computation of compliance relationships.

Two loading conditions will be utilized:

(1) unconfined axial compression

(2) axial extension.

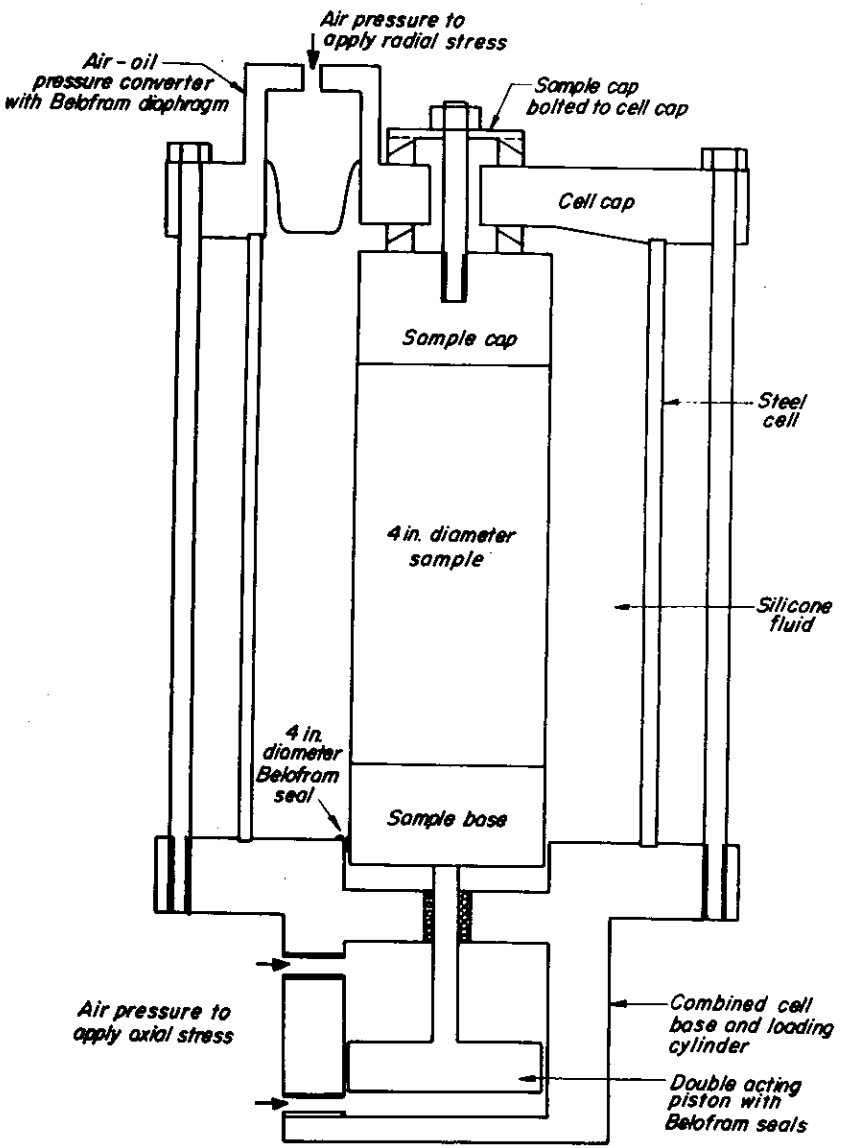

Fig. B-1 — Triaxial apparatus permitting independent variation of axial and radial stresses.

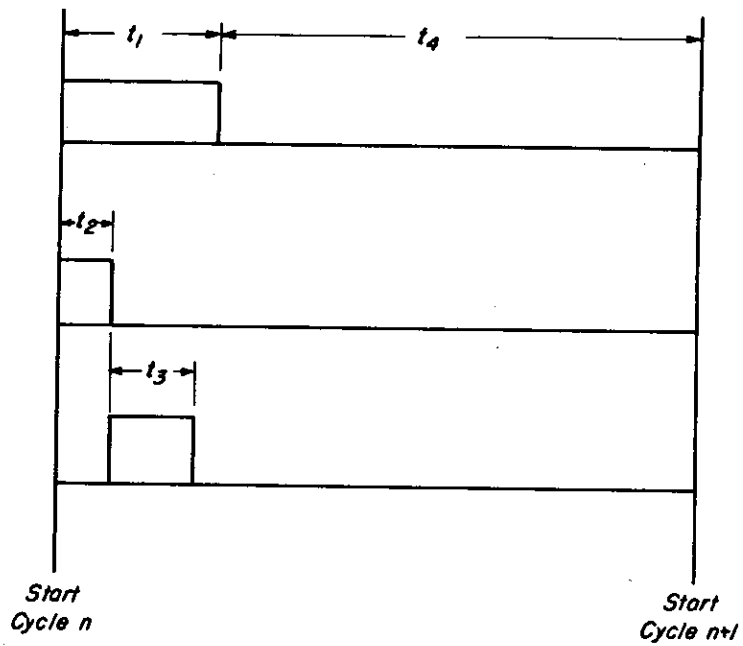

$$\text{Cycle time} = t_1 + t_4$$

$$t_2 + t_3 \leq t_1$$

Fig. B-2 — Timer signal outputs.

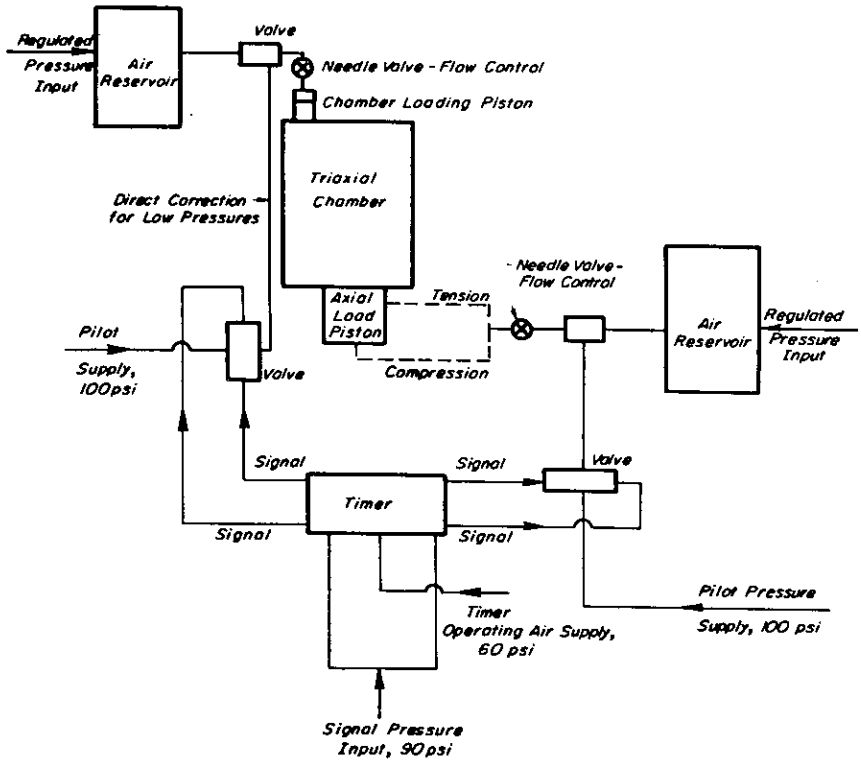

Fig. B-3 — Schematic diagram of triaxial loading system for repetitive loading tests.

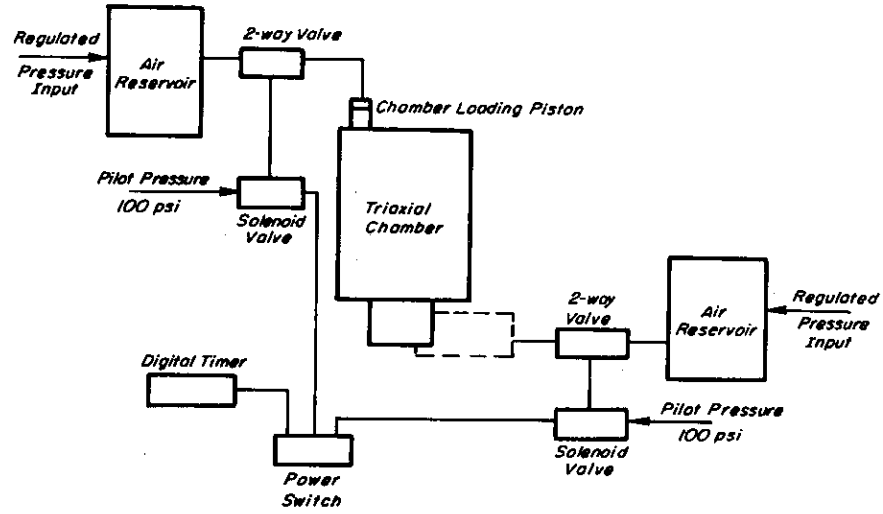

Fig. B-4 — Schematic diagram of triaxial loading system for creep tests.

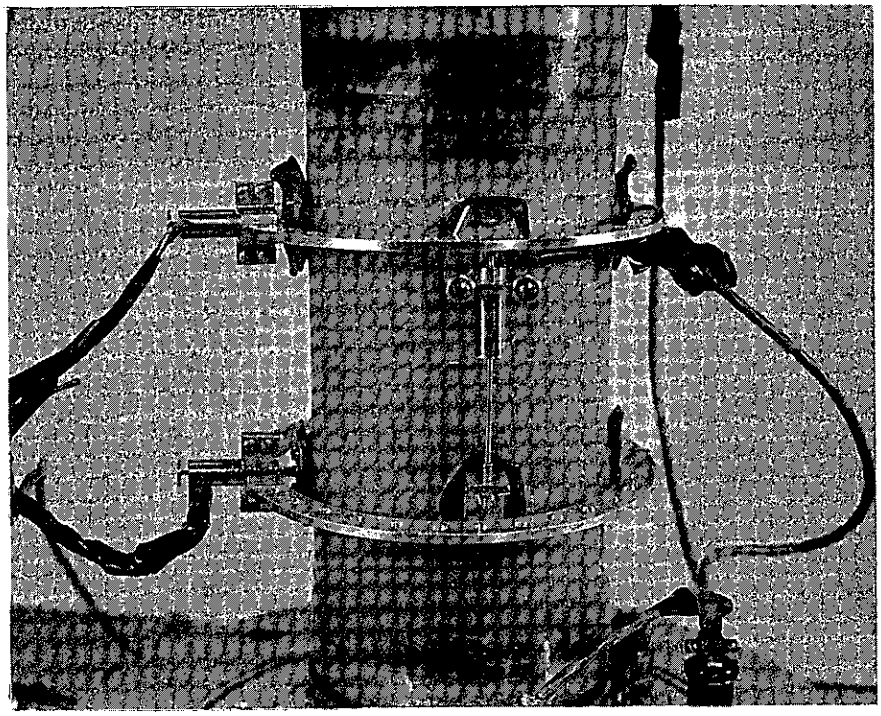

Fig. B-5 – Photograph of deformation measuring device.

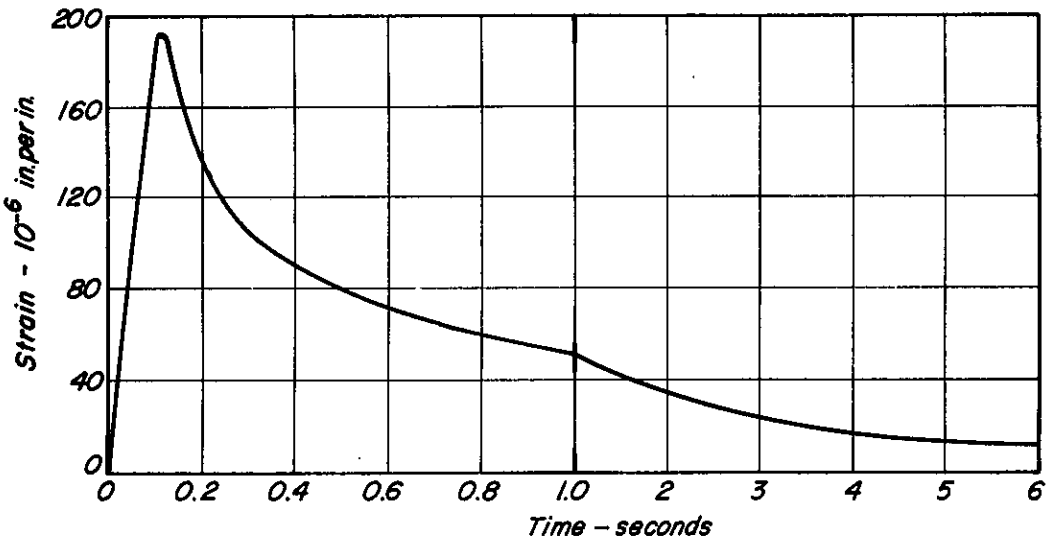

Fig. B-6 – Deformation recovery time in unconfined axial compression, T = 100° F.